DEGREE PROJECT IN VEHICLE ENGINEERING,
SECOND CYCLE, 30 CREDITS
STOCKHOLM, SWEDEN 2019

Functional Testing of the Electrical Power System of the MIST Satellite

STEFANO BARRA

KTH ROYAL INSTITUTE OF TECHNOLOGY
SCHOOL OF ENGINEERING SCIENCES

Any sufficiently advanced technology is indistinguishable from magic.

- Arthur C. Clarke

Abstract

The Electrical Power System is the key subsystem for the survival of the satellite. It not only supplies power to the satellite by keeping the battery adequately charged, but it also provides crucial fault detection and recovery functions. The target of this thesis work is to characterize and test all the functionalities of the EPS of the MIST satellite in realistic operational conditions through the implementation of hardware and software simulators. Such a comprehensive framework is based on a MATLAB software, the MIST flight hardware, as well as Solar Panel Simulators and Arduino-based dummy loads created by previous students in the project. These tools are used to integrate all these elements into an easy-to-use simulation environment that very closely mimics conditions in actual orbital flight and that can be used as a model for such simulations in similar satellite projects. The purpose of the simulations in this environment is to verify that the planned flight profile of the satellite is correct and safe, especially from a power subsystem point of view.

Sammanfattning

Elkraftsystemet är det viktigaste delsystemet för överlevnaden av satelliten. Den levererar inte bara ström till satelliten genom att hålla batteriet tillräckligt laddat, utan ger också avgörande feldetekterings- och återhämtningsfunktioner. Målet med detta avhandlingsarbete är att karakterisera och testa alla funktionaliteter under realistiska driftsförhållanden för EPS genom implementering av en hårdvaru- och mjukvarusimulering av MIST-satelliten och dess flygmiljö i omloppsbana. En sådan omfattande ram kommer att baseras på en MATLAB-programvara, MIST-flyghårdvaran samt solpanelsimulatorer och Arduino-baserade dummy-laster skapade av tidigare studenter i projektet. Dessa verktyg används för att integrera alla dessa element i en lättanvänd simuleringsmiljö som är mycket nära besläktad med den faktiska omloppsflygningen som kan användas som modell för sådana simuleringar i liknande satellitprojekt. Syftet med simuleringar i denna miljö är att verifiera att den planerade flygprofilen för satelliten är korrekt och säker, särskilt ur ett energisubsystemssynpunkt.

Acknowledgements

I would like to express my gratitude to my supervisor Theodor-Adrian Stana for his guidance and support during the thesis work. I would also like to thank Sven Grahn, Prashant Yadav, Hosam Hakeel and Andrii Berezovskyi for their help throughout the year.

Contents

List of Figures

List of Tables

Acronyms

BOB BreakOut Board

CSKB CSKB

DoD Depth of Discharge

EGSE Electric Ground Support Equipment

EPS Electric Power System

ESD ElectroStatic Discharge

GOSH GOmspace SHell

HDRM Hold Down Release Mechanism

IGIS ISIS Generic Interface System

iMTQ ISIS Magnetotorquer

iOBC ISIS On Board Computer

MCU Measurement Control Unit

MIST MIniature Student saTellite

MPPT Maximum Power Point Tracker

MTI MIST Test Interface

SPS Solar Panel Simulator

TRXVU ISIS Transceiver, UHF Transmitter and VHF Receiver

Chapter 1

Introduction

1.1 The CubeSat standard

CubeSats are a category of nano-satellites constituted by one or more cubes, called units, of 10 cm sides and a maximum weight of 1 kg [1]. The CubeSats have standard size and requirements, which allows their development to be simpler and cheaper than bigger satellites, making them the preferred design choice for small organizations, such as universities. The usage of CubeSats for scientific mission has seen a fast increase in recent years [2], resulting in a growing demand for CubeSat components. Figure 1.1 shows a 1U CubeSat with solar panels on each side.

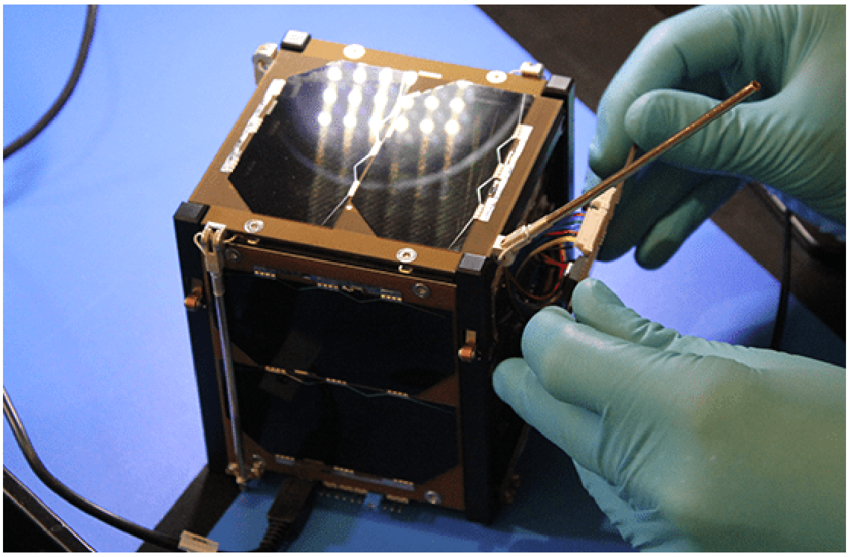

Figure 1.1: A CubeSat under assembly

1.2 The MIST project

The MIST is a professionally run student project aimed at developing a 3U CubeSat [3], designed to carry several experiments to space. Every phase of designing, building and testing of the CubeSat has been carried out by different student teams, involved in the project for a semester or one year. Most of the experiments that will fly with MIST have been designed by several KTH departments, while others come from private companies. The experiments are:

- **NanoProp**: a propulsion experiment provided by NanoSpace,
- **Piezo LEGS**: a piezoelectric motor provided by Piezomotor AB, in Uppsala,
- **CUBES**: an innovative radiation detector proposed by Particle and Astroparticle Physics group, Dept. of Physics, KTH,
- **SiC**: a space-grade semiconductor proposed by the Integrated Devices and Circuits group, ICT school of KTH,
- **SEUD**: an SEU detector proposed by the Department of Electronic Systems, KTH.
- **Camera**: Designed to obtain an image of Sweden from space.

The CAD model shown in Figure 1.2 displays the subsystems configuration of the satellite. The solar panels and the antennas have been removed to show the internal units.

Figure 1.2: The MIST CAD model

1.3 Functional Testing

The malfunctioning of the Electrical Power Systems is the cause of a large majority of failures in Cubesats [4].

Functional testing is a type of black-box testing used to verify the functionalities of a software or hardware product [5]. The purpose of functional testing is to minimize the risk of failure of a component, and to verify that its behaviours in different situations are known. Testing of a component or a system, especially a complex one such a CubeSat, is a necessary part of a project, and it's most effective when the system's requirements are well known. This knowledge allows the tests to be based on the expected functionalities of the systems. Understanding the environment that the system has to operate in is necessary to design test cases that will analyse when a failure could occur.

Chapter 2

Background

2.1 Subsystems of the MIST satellite

The MIST satellite is composed of the structure, the subsystems and the payload [6]. These are separated in three different units, referred as:

- Top Stack,
- Middle Stack,
- Bottom Stack.

Specifically, the Top Stack and Bottom Stack integrate the experiments, described in Section 1.2, while the Middle Stack accommodates the subsystems. These units are held together by the structure.

The MIST satellite subsystems include:

- **OBC**: *On Board Computer*, is the unit which provides processing capability and contains the satellite's avionic and flight software [7]. It controls the satellite's attitude, telecommands execution, on-board time distribution, experiment handling and memory storage. It was developed and manufactured by ISIS.
- **EPS**: *Electrical Power System*, constituted by a Battery Pack (BP4) and a Power Distribution Unit (P31us), it converts the input power from the solar panels to charge the batteries and to power the satellite [8]. It is provided by GomSpace.

- **TRXVU**: *ISIS Transceiver, UHF Transmitter and VHF Receiver*, is a radio system used to communicate with the ground station, receive telecommands and transmit telemetry and science. It uses two sets of dipole antennas, one for transmitting and one for receiving, deployed by a one-shot mechanism, called AntS. It is provided by ISIS.

- **iMTQ**: *ISIS Magnetorquer*, 3-axis coils and control board, used for attitude control by interacting with Earth's magnetic field. It is provided by ISIS.

- **IGIS**: *ISIS Generic Interface System*, a device used for harnessing management and to provide umbilical ground connections. It is provided by ISIS.

2.2 The Electrical Power System

One of the most important subsystems in the MIST satellite, as in any type of satellite, is the electrical power system or EPS. The main role of the EPS is to provide a satellite with power during the flight. Power is obtained directly from the solar panels during sunlight, and from the battery pack during eclipse [8]. The MIST EPS is composed of two units: the Power Distribution Unit (P31us) and the Battery pack (BP4), shown in Figure 2.1a and Figure 2.1b, respectively.

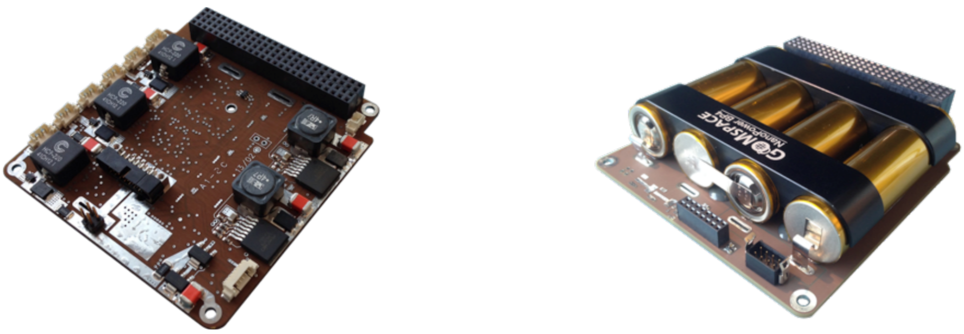

(a) P31us

(b) BP4

Figure 2.1: EPS modules [8]

A scheme of the EPS is shown in Figure 2.2. This diagram shows the power distribution, starting from the photovoltaic cells of the solar panels (left) toward the battery pack and the power distribution matrix (right). The dotted lines indicate a single item of the EPS telemetry and where it is measured. The power distribution matrix allows direct powering of the components, such as the experiments, via the *switched power lines*, while the 3V3, 5V and Vbat lines power the CSKB directly. The MCU (bottom) controls the EPS and provides communication with the rest of the satellite (via I^{2}C) or with the ground equipment (via the GOSH).

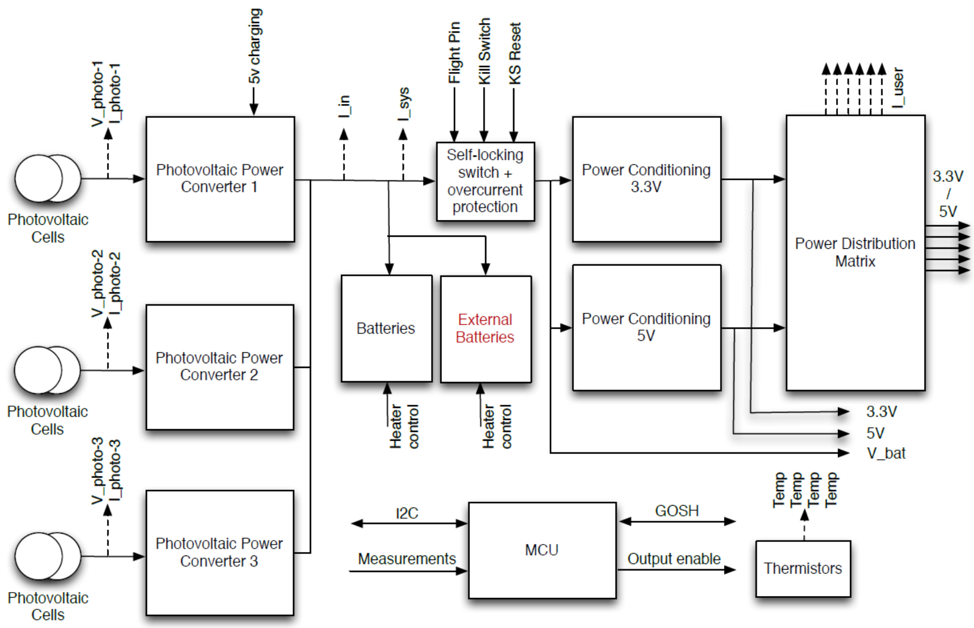

Figure 2.2: EPS block diagram

The EPS holds several critical functions for the satellite operation. The following subsections describe some of the main functionalities, used for the functional testing framework.

2.2.1 MPPT

The EPS can manage the input voltage and current using the MPPT method to obtain the maximum available power from the solar panels. The MPPT is an algorithm commonly used in solar panels technologies that selects the input current and voltage corresponding to the knee of the IV curve, i.e. the point of maximum power.

The IV curve, showed in Figure 2.3 is used to characterize the load profile that a solar panel can provide. Since the input current provided by the solar panels is variable due to the satellite's movement along its orbit and shadowing phenomena, the EPS has to continuously shift the input voltage and current to obtain the maximum power. The IV curve is calculated from the characteristics of the p-junctions of the solar panels [9], showed in Equation 2.1:

$$I = I_L - I_0 \left[\exp\left(\frac{qV}{nkT} \right) - 1 \right], \tag{2.1}$$

where I is the current, I_L is the light generated current, I_0 is the dark saturation current (usually small), q is the electron charge, V is the voltage, n is an ideality coefficient, kT is the Boltzmann constant times the operating temperature [9]. Assuming that the exponential term in Equation 2.1 is much greater than 1, as it usually is, the equation can be rearranged in terms of voltage:

$$V = \frac{nkT}{q} ln \left(\frac{I_L - I}{I_0} \right), \tag{2.2}$$

that can be computed to obtain the graph shown in Figure 2.3. The points where the I and V go to zero represent, respectively, the short circuit current $I_{S/C}$ and the open circuit voltage $V_{O/C}$. It also shows that the "knee" of the curve corresponds to the maximum available power P_{max}, obtained by the product between current and voltage:

$$P_{max} = I_{mmp} V_{mmp}. \tag{2.3}$$

The MIST satellite employs different combinations of solar cells in series

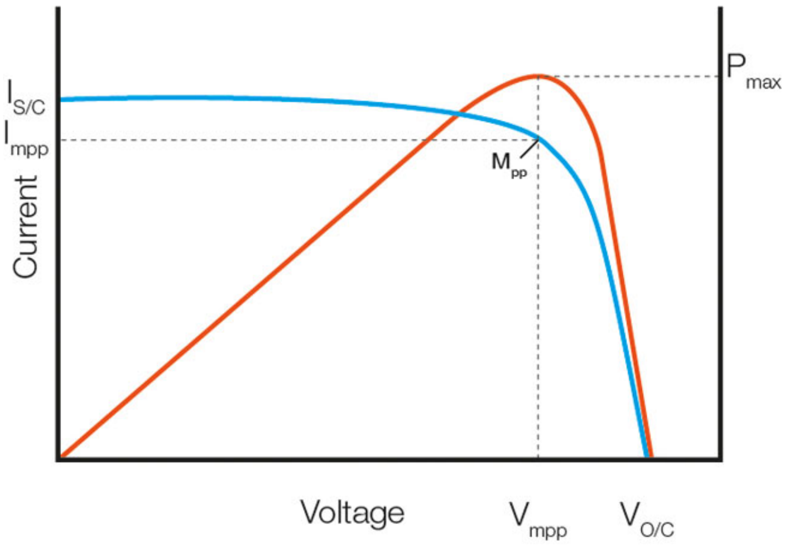

Figure 2.3: A typical IV curve for one solar cell

and parallel. The configuration was selected to obtain the maximum power with the given solar panels placements [10], and is shown in Figure 2.4.

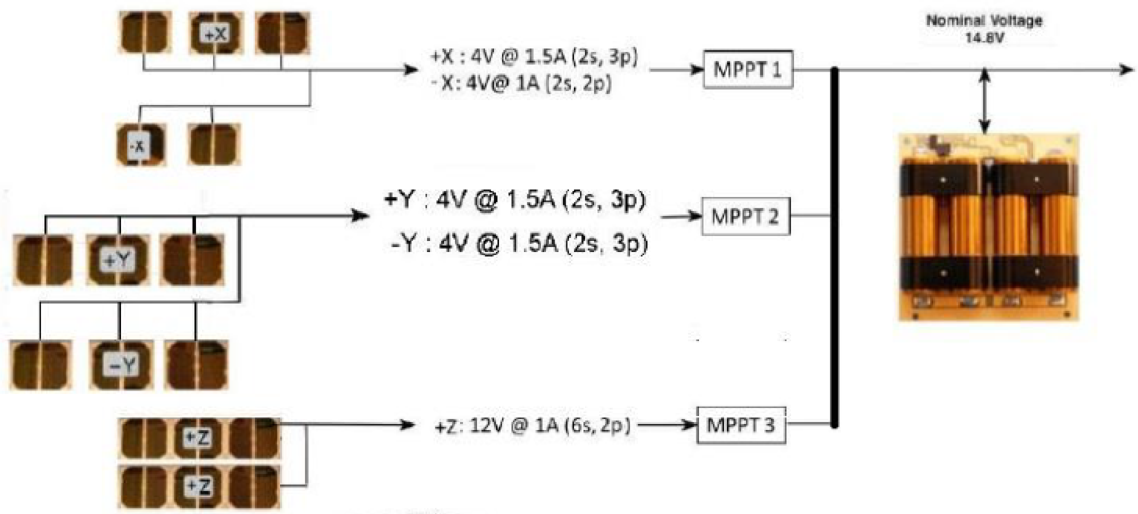

Figure 2.4: Current solar cells configuration in the MIST

The use of three separate cells configuration, one for each side of the satellite, requires the use of three independent MPPT. Each of these is controlled autonomously by the EPS, and the tracking algorithm can be engaged or disengaged as necessary.

2.2.2 Watchdog Timer

In case the satellite stops responding, the P31us can reset it via the implementation of watchdog timers. The WDT operates by power-cycling the iOBC if no communication has been received after a custom interval of time [8]. The simplified schematic of a watchdog algorithm is shown in Figure 2.5.

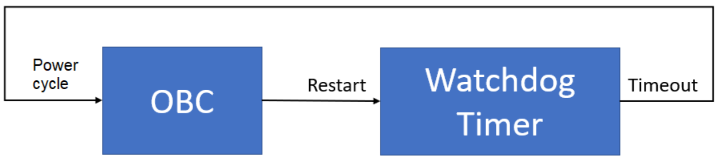

Figure 2.5: Watchdog timer operation

Figure 2.5 describes the watchdog algorithm in detail:

- If the OBC is operative, it *kicks* the watchdog, restarting the timer,
- If the OBC is not operative, it can't kick the watchdog. When this happens, the watchdog timer reaches a timeout, triggering a restart of the OBC.

The P31us also implements a dedicated watchdog timer, where the reset is triggered by a specific command. In can be used in connection with the ground station: if no communication has been received during a ground station pass, the satellite is power-cycled. [8].

2.2.3 Electric Protection

The EPS contains electronic protection circuits that allow the satellite to withstand out-of-nominal power input or output. These can be caused by multiple factors, such as power surge from the solar panels or the experiments, as well as accidental short circuits. The electronic protection circuits also prevent the battery from reaching a critical charge status, both in terms of low and high voltage [8]. These circuits are described in detail in Section 4.3. Testing of these circuits is of vital importance, since they are part of the first set of defences of the EPS from electric failures. Particular attention must be paid to the methods the EPS adopts to prevent failures, since its behaviour could cause consequential unexpected failures, or block the satellite in an idle state without means for its recovery.

Chapter 3

Testing Framework

The MIST satellite's scientific payload consists of 5 experiments that have different requirements in terms of operation time and power consumption. The scheduling operations of the experiments have been studied in the system engineering simulations [6]. One of the main roles of the functional testing is to verify that these simulations match with the hardware specifications of the satellite. Specifically, the functional testing of the EPS aims at:

- Verifying the power budget analysis,
- Measure the DoD of the battery pack,
- Checking that the payload power demands do not interfere with the EPS functionalities.

To test these cases, the satellite needs to be tested on a system level, to understand the effect that different subsystems can have on each other. At the same time, control of every subsystem is required to separate eventual effects showing on the tests. The testing can be performed with the design of a *test framework*. The hardware component of this framework is a legacy of the project from previous students team, and it can be divided into three separate systems:

- MIST Flatsat Setup,
- Solar Panels Simulators (SPS),
- Experiment Simulators (or Maltuinos).

The MIST Flatsat Setup is a configuration of the satellite, where all the subsystems are stacked in an horizontal fashion, to provide a ready access to the CSKB and to allow easy visual inspection of every component. More information can be found in Chapter 6. A schematic of the full layout is shown in Figure 3.1.

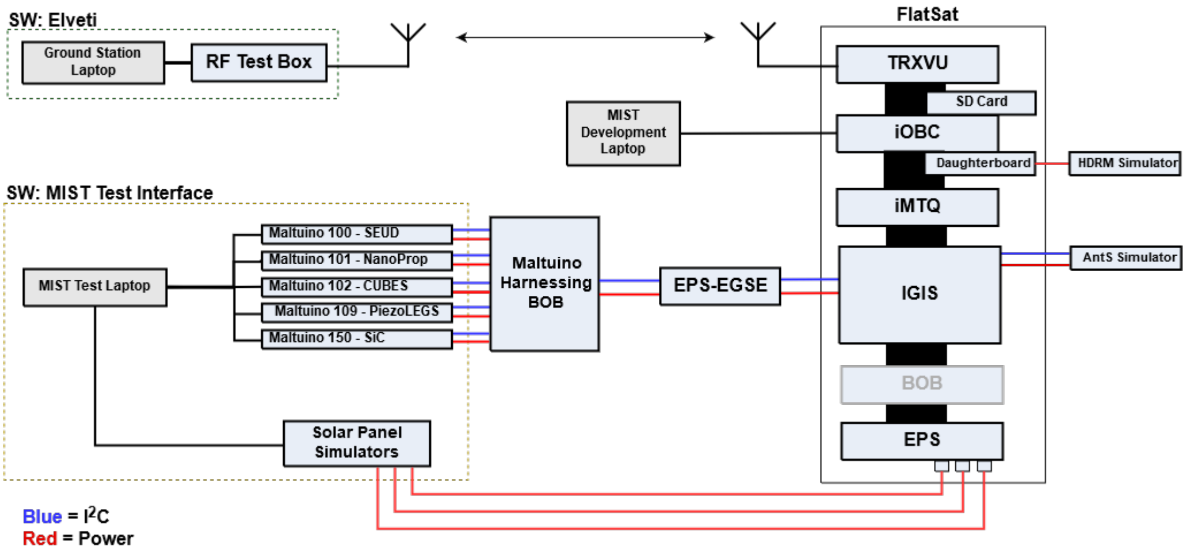

Figure 3.1: Schematics of the MIST Testing Framework

The actual hardware set-up, as assembled in the MIST Integration Lab, is shown in Figure 3.2.

3.1 Experiment Simulators

In the current state of the project, most of the flight hardware is available for testing. This includes the components of the subsystem stack. However, the satellite's payload is not available for functional testing, as their development is still in progress. For this reason, the power requirements for the payload are not definitively set, as they might change during the design of each experiments. It follows that the expected schedule of activation of the experiments might change several times before being confirmed.

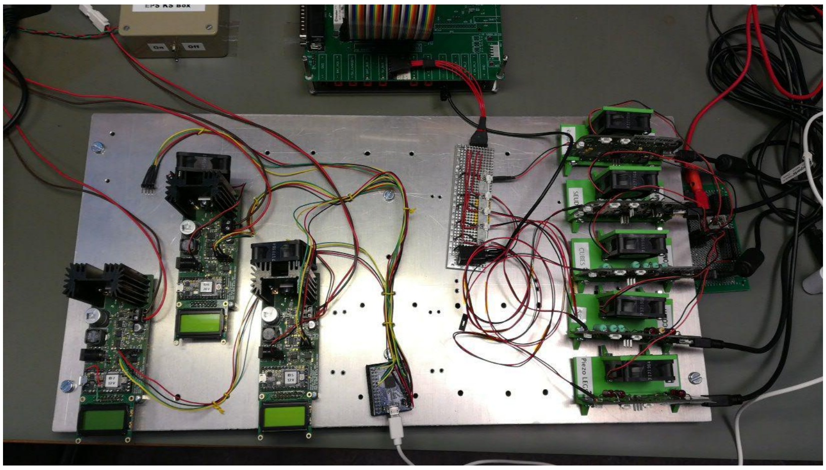

Figure 3.2: MTF Hardware setup

To study the behaviour of the EPS in different power draw conditions, the experiment had to be simulated using *dummy loads*, referred to as experiment simulators, or Maltuinos [11]. One of these boards is displayed in Figure 3.3.

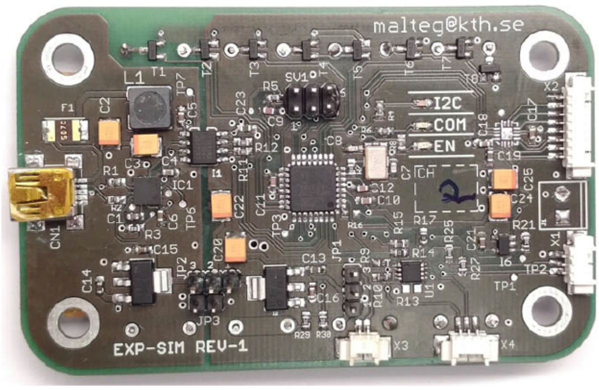

Figure 3.3: Top view of the Experiment Simulator board

The experiment simulators are Arduino-based boards that draw power from the EPS, effectively simulating the power consumption of an active experiment. They achieve this by dissipating power over a set of 8 resistors, placed at the bottom side of the board. The voltage is kept constant (either 3.3 V or 5 V) while the current changes depending on the resistor value. Each resistor is controlled by a fast-switching FET (DMG3414U) [11], that allows the board to activate or deactivate each resistor individually, placing them in parallel to the

EPS. The Arduino-based software loaded on the experiment simulator board can handle a total of 32 load cases (named from *L0* to *L31*) that correspond to state of the transistors, in binary. Some examples are shown in Table 3.1.

Load Case	**Binary Value**	**FETs State**	**Explaination**
L0	0b00000	All FETs OFF	Open circuit, no power draw
L1	0b00001	FET 1 ON	Only resistors connected to FET 1 are connected to the circuit
L2	0b00010	FET 2 ON	Only resistors connected to FET 2 are connected to the circuit
L3	0b00011	FET 1 & 2 ON	Resistors connected to FET 1 and FET 2 are connected to the circuit
...	...	...	...
L31	0b11111	All FETs ON	All resistors connected to the circuit, maximum power draw

Table 3.1: Load case, FET and relative resistor configuration examples

More details about the hardware and on how the FET controls the resistors can be found on the experiment simulators PCB schematics, available in the Appendix 6.1. The load cases (*L0* to *L31*) that control the FET states can be activated by the experiment simulators using the serial communication of the board. Simply by setting up a command window and sending the serial command *L* followed by a number from *0* to *31* will set the experiment simulator power load corresponding to the connected resistors.

The serial communication via command window can be used during debug or for simple load case scenarios, since such command would only activate the load, without allowing an automated control of the load profile, i.e. load variation over time. This requires the development of an external software, the MTI, described in Section 3.4.

The development of this thesis work required the assembly of these Experiment Simulators, including soldering of a shunt and a voltage divider resistors, for voltage and current reading, respectively. These values are collected by the Experiment Simulators and sent via serial communication by request. Figure 3.4 shows the Experiment Simulators assembled and deployed on the MIST test bench, with their experiment identifier.

Finally, a support for the board and cooling fans was designed using a CAD tool and manufactured with a 3D printer. The vertical placement was chosen for efficient cooling of the resistors to avoid damages to the laboratory ESD protection mat. Each board simulates a different experiment, recognizable by each name tag.

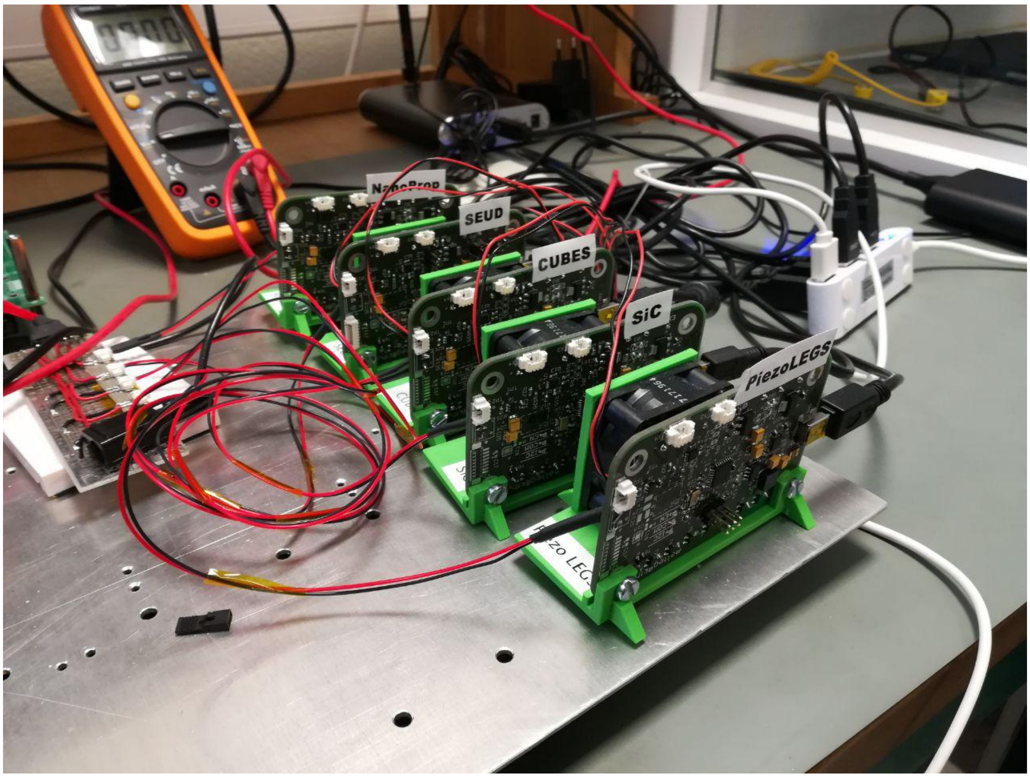

Figure 3.4: The experiment simulator boards

3.2 Solar Panels Simulators

The Solar Panel Simulators (SPS) are devices designed and manufactured to provide input power to the satellite, much like the real solar panels [12]. They have been developed by Gustav Pettersson during his work in the MIST project, and are now used for functional testing purposes.

Their principle of operation is to draw a constant current at a fixed voltage from three separate power outlets. Two of these are at 12 V, and one is at 24 V, to simulate the three solar panel's inputs to the MPPT. A Teensy board is used to manage the amount of power to dissipate, varying both in current and voltage. The extra power is then dissipated on a high-power transistor, provided with active cooling. The assembled SPS boards are shown in Figure 3.5.

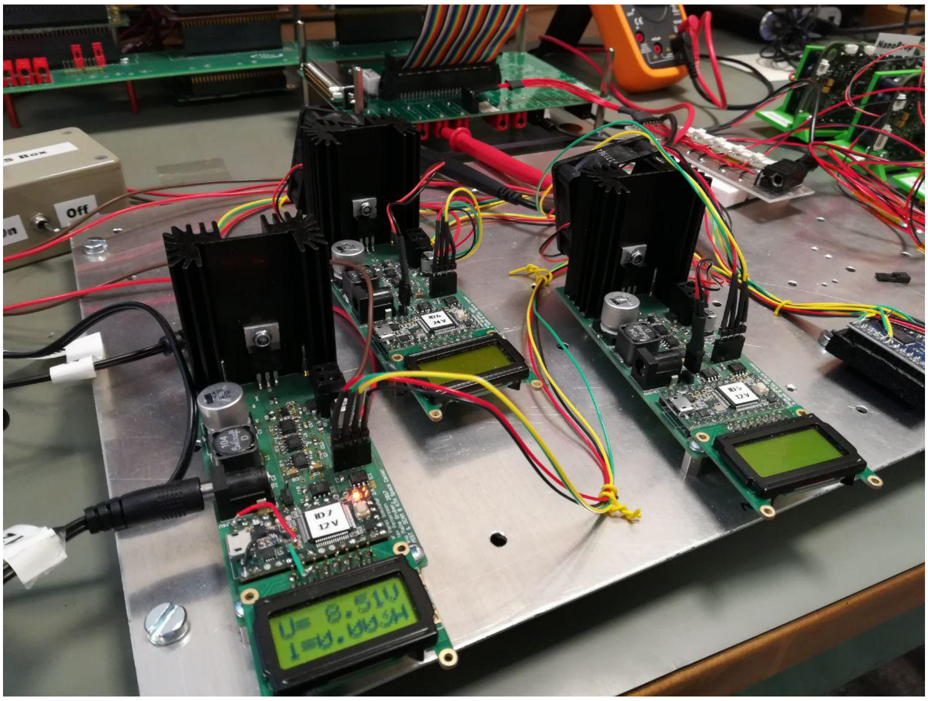

Figure 3.5: The Solar Panel Simulator boards.

To be as close to reality as possible, the SPS manages both current and power independently, simulating the real behaviour of the solar panels when exposed to sunlight.

The Teensy boards are controlled by a MATLAB software, available on GitHub [13], that allows both a manual control of the input power (for charging purposes) and an automated orbital simulation of the input power. The power profiles that the SPS can simulate are computed by the MATLAB software in several scenarios, and a combination thereof, such as:

- Nominal attitude or tumbling,
- Deployed or undeployed solar panels,

- High or low solar flux (winter and summer case).

Each of these cases can be modified according to the test case.

Finally, the SPS can be calibrated to output the *real* power, taking into account the non-idealization of the solar panels used in MIST. The calibration process is described in the SPS manual [13].

The standard power profile used in the basic simulation is shown in Figure 3.6. These curves display the power variation during the course of one full orbit, starting 10 minutes before entering sunlight. Each curve represents the input power selected by the MPPT, thus they depend on the angle of the sun on the solar panels, which changes during the course of the orbit.

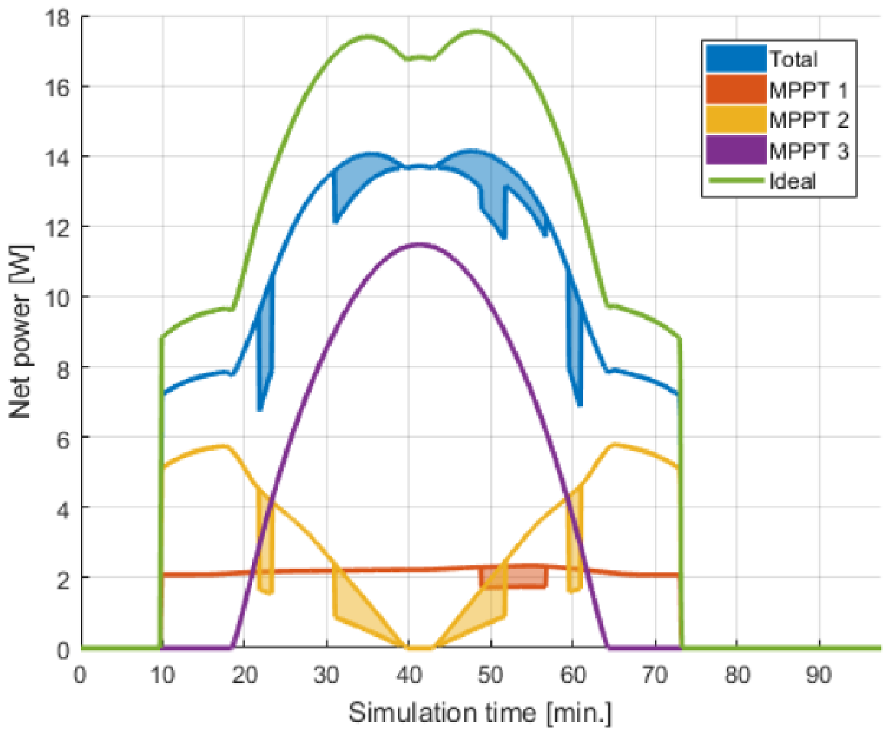

Figure 3.6: Example of a power profile simulated by the SPS

3.3 The EPS-EGSE

The EPS-EGSE is an electronic board developed by ISIS and it's used for functional testing operations. It provides an interface to standard test equipment, like laptops and bench power supplies, during stand-alone testing [14]. It allows to directly interact with the pins of the CSKB without contact with the flight hardware. It can also provide communication with the I^{2}C bus. For the functional testing of the EPS, it was used mainly to handle the switched line power. These lines were used to power the experiment simulators. By providing access to the 3.3 V, 5 V and V_{bat} lines, it allowed to monitor the status of the battery voltage with an external tool, for redundant measurement. An example of implementation of the EGSE in the satellite functional testing framework, also used in the current setup, is shown in Figure 3.7.

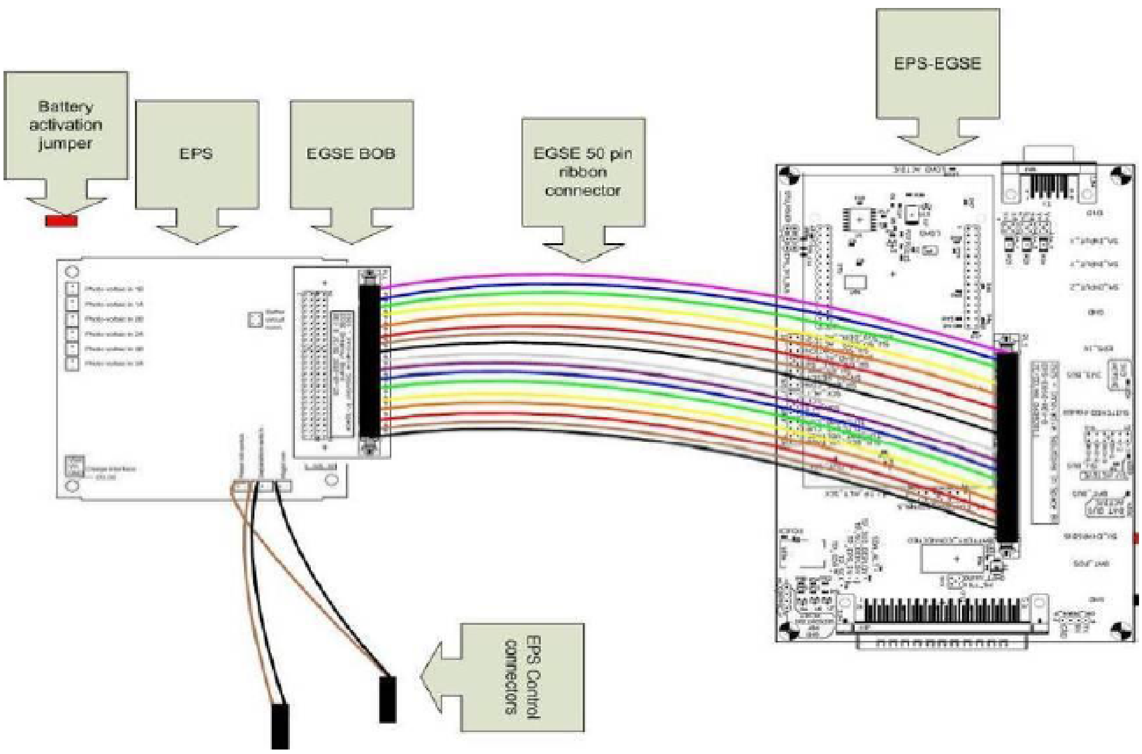

Figure 3.7: EPS-EGSE connection to the EPS [14]

The actual EPS-EGSE hardware is shown in Figure 3.8, on top left, and the switched lines connections and BoB in the center. Each switched power line is connected to the experiment simulators, on the bottom left. More information on this setup is available in the MIST documentation [15].

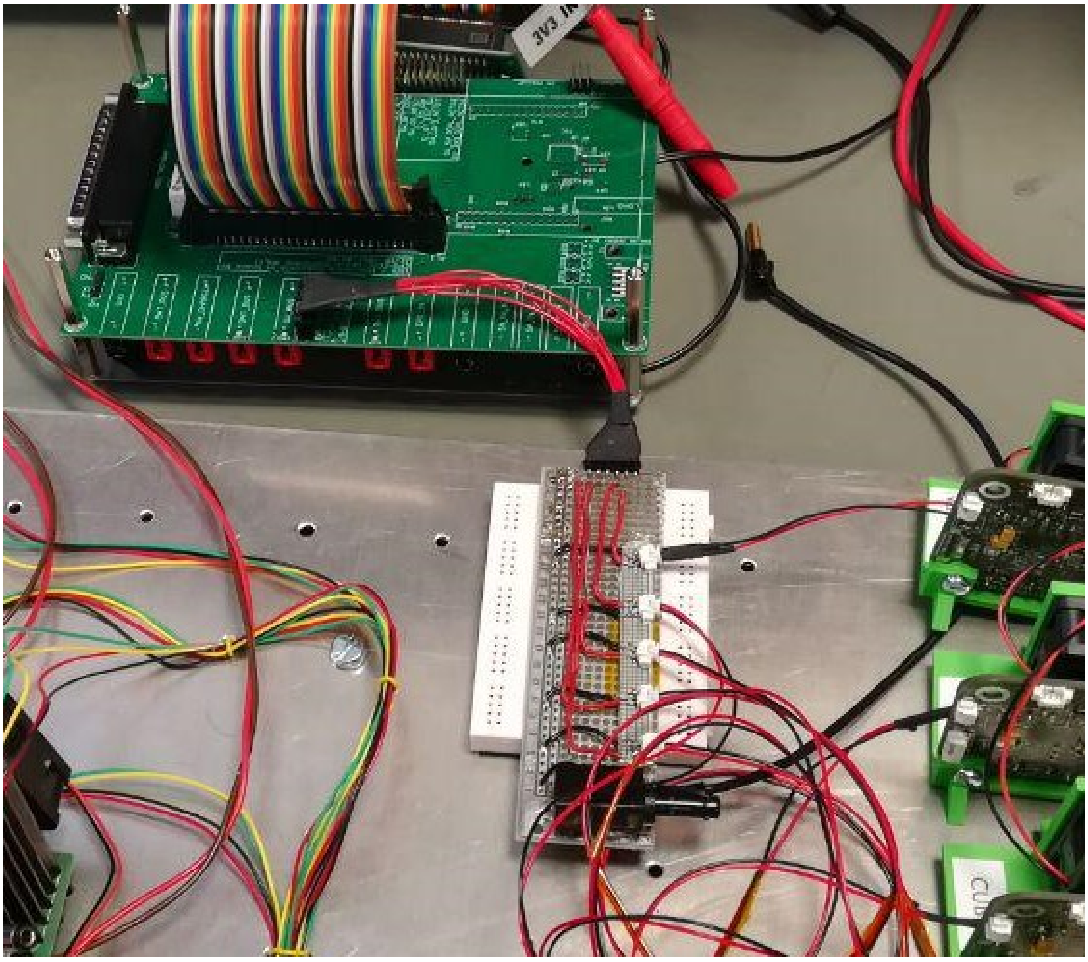

Figure 3.8: EPS-EGSE hardware and switched lines

3.4 MIST Test Interface

The MIST Test Interface is a MATLAB based software used to manage the loads of the experiment simulators. It allows both the selection of a constant load and the set-up of a scheduled power profile. The software is provided with a GUI to allow an easier management of the test, and it is designed to be easy to use and compatible with different machines. A preview of the MTI GUI running a test is shown in Figure 3.9.

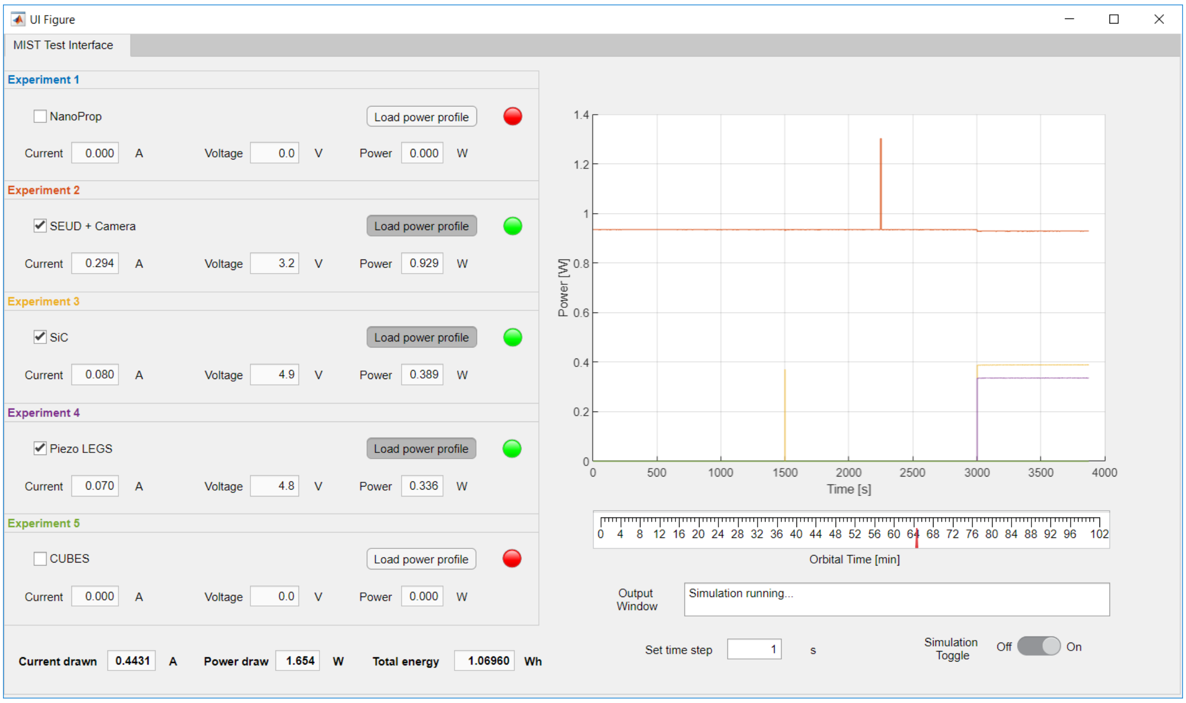

Figure 3.9: GUI of the MTI software

The MTI software can retrieve telemetry values in real time from the experiments simulators, such as voltage and current draw, for monitoring their status and for logging purposes. These values are displayed and updated in real time near each experiment, next to an icon showing the connection status. The bottom line shows the total current and power draw currently applied to the EPS, followed by an estimated energy draw. The right side shows a live updated graph of the power, as measured by each experiments. This can be used to identify the power switches, unexpected oscillations and for monitoring the functionality of each experiment simulator. It is important to point out that the values shown do not represent the *real* total power consumption, but only an estimation based on the values measured by the experiment simulators. They should be used primarily to check the test's progress, identify anomalies or failures. Nonetheless, these telemetry values can be compared to the satellite's measurements of power draw to obtain the wiring and connector's losses. More details are presented in the Results chapter and in the Appendix 6.2.

The flowchart of the MTI software is shown in Figure 3.10, where the red blocks represent the user input, the blue are processes, the green is a memory storage writing and the yellow represent the switches and terminator.

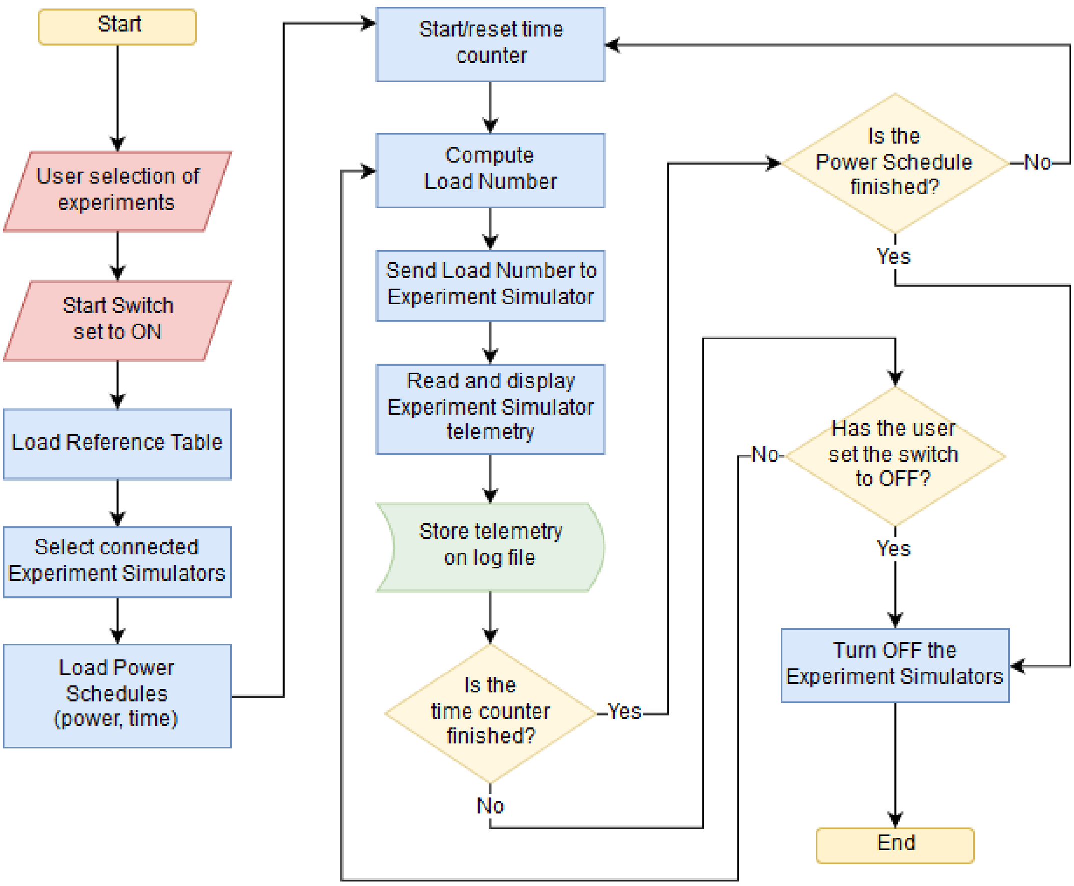

Figure 3.10: Flowchart of MTI

The flowchart in Figure 3.10 illustrates that the functional flow of the MTI can be separated in three sections, listed below:

- Start-up (left blocs),
- Communication with the experiment simulators (central blocs),
- Exit conditions (right blocs).

In the *Start-up* sections, user can select the experiments to use during the test. This selection is done by choosing the experiment, and by loading a table file containing each experiment's schedule. Figure 3.11 shows an example of such table, in a test where only the experiment NanoProp is used, during two orbits.

	A	B	C
1	**t [s]**	**P [W]**	
2	1700	1.7	Tank Pre-Heating
3	100	2.7	Thruster Pre-Heating
4	600	8.7	Thrust
5	10700	0	Idle
6	1700	1.7	Tank Pre-Heating
7	100	2.7	Thruster Pre-Heating
8	600	8.7	Thrust
9	10700	0	Idle

Figure 3.11: Example of a power schedule

By loading the power schedule table the MTI creates a vector of time counters relative to each power value. The MTI then continues sending the same power value command to the Experiment Simulators until the time counter expires. It then proceeds by sending the power value commands, until all the counters are reached or the user stops the simulation. Note that, if multiple experiments have to be used in a single test, the time counters should be exactly the same in each table file. The reason for this lies in a MATLAB limitation of allowing only one time counter per session which prevents the use of separate and independent timers. For this experimental setup, the power schedule tables have already been compiled and can be used as examples for the next tests.
Following the user switch button to ON, the MTI loads a reference table (compiled during the assembly of the experiment simulator), shown in Table 3.2,

and matches the input power with the closest value available of the board. Since the experiment simulator can only handle 32 values of power, any intermediate input power value is chosen via a linear interpolation.
The reference table cut-out in Table 3.2 can be helpful to understand what power dissipation each experiment simulator can provide, also showing the value of current and the corresponding command used in the serial communication (L1 to L31). This can be useful to control an experiment simulator manually, using a serial port.

L	I [A]	R [Ω]	P [W]
0	0	0	0
1	0.064	78.125	0.320
2	0.322	15.125	1.610
3	0.386	12.953	1.930
4	0.243	20.576	1.215
5	0.307	16.287	1.535

Table 3.2: Reference table for NanoProp

Once the start-up is completed, the MTI starts sending commands to the experiment simulators in the *Communication* section. The boards have an on-board software that is programmed to send telemetry data and switch transistor states via serial command. Thus, the MTI automatically matches the requested power load to the appropriate command (see Table 3.1) and sends it via the serial port. As shown in Figure 3.10, the MTI follows by sending the commands relative to a telemetry request, and then proceeds to register, display and save these values. A list of the commands used by the MTI is shown in Table 3.3.

Finally, the *Exit Condition* section contains a sequence of if-statements that allow the process to exit the main loop, resetting the time counter if the sequence is not over, otherwise closing the logger file and preparing for a new test session. The MTI is designed to handle several tests in the same session, without having to re-load the reference tables or power schedule. These can be modified via an external application, and the MTI adds the modified queries at the end of each test. It is also possible to add more experiments and to stop the test at any time.

Serial Command	**Explanation**	**Example Answer**
L0	Set power draw to 0	No answer
L#	Set load case # (from 1 to 31)	No answer
w	*Who*	Maltuino
i	*ID*	101
v	*Version*	v1.0
c	Current reading	300 mA
V	Voltage reading	5.00 V
h	Display available commands	Command list

Table 3.3: Experiment Simulator commands

Chapter 4

Test Procedures and Results

4.1 Test Procedures

The following section illustrates the standard test procedure used, followed by the results obtained for each test. These can be used as a guide for the test framework described in this thesis. The design of this procedure was outlined with the help of the ECSS requirements for testing [16], but the detailed instructions were compiled after simulating each test, noting the critical steps in the attempt to avoid any dangerous conditions. The instructions are thus subject to future reviews and updates, and the most updated version can be found in the MIST Functional Testing work folders (M631). At the time of the writing, this thesis is the most updated document available of the test procedure. The activation schedule of the experiments used in the tests follows the system budget documentation [17], which is also subject to future changes. Thus some of the results showed in this chapter might have validity only when referred to the power schedule used. In Table 4.1 the testing and monitoring process is shown, while the complete list of instructions are available in Appendix 6.

4.2 Post-Processing

For simplifying the verification and the analysis of the test results, a MATLAB-based post-processing tool was developed. If follows the process of data-retrieval from the iOBC logger, conversion and storage of the telemetry, described in Chapter 4. The purpose of this tool is to give an immediate visual outcome of the test result, such as the Battery Voltage, Input and Output currents, voltages and power, as well as the switched lines status. These data are only a small part of the telemetry saved by the iOBC during the tests, but can serve to give an immediate feedback on the test result, allowing the user to validate the test outcome as soon as the test is completed. It can be also used for a first iteration of data analysis. The tool combines the obtained data to display a graph, however it can also apply a smoothing algorithm on the visualized data (without modifying the original data matrix), such as a moving average with different step size for removing spikes, caused by overflow, or high-frequencies noise. This tool was used to generate the figures shown in Chapter 4, and can be improved by the next Functional Test team to include more graphics, more filtering options, or to integrate the data splitting algorithm.

Experiment Simulators	**Solar Panels Status**	**Attitude**	**Solar Flux**
No Experiments	Deployed	Nominal	Best Case
No Experiments	Undeployed	Tumbling	Worst Case
SEUD, CUBES	Deployed	Nominal	Best Case
SEUD, CUBES	Deployed	Nominal	Worst Case
SEUD, PiezoLegs, SiC	Deployed	Nominal	Best Case
SEUD, PiezoLegs, SiC	Deployed	Nominal	Worst Case
SEUD, NanoProp	Deployed	Nominal	Best Case
SEUD, NanoProp	Deployed	Nominal	Worst Case
Fast Charge	Maximum input power	N/A	N/A
Fast Discharge	No input power	N/A	N/A

Table 4.1: Experimental Test Groups

4.3 Test Group 1 - EPS Functionalities

4.3.1 Test Procedure

The first set of test is aimed at verifying the basic functionalities of the EPS. Specifically:

- Maximum output current protection (2 A),
- Maximum battery voltage protection (16.6 V),
- Minimum battery voltage protection (13.8 V).

These tests allows to verify that the basic protections of the EPS functions properly. The values to be tested have been selected from the EPS manual [8], however it is possible to modify the maximum and minimum battery voltage value via software.

The test is executed in three different sub-tests. The first, aimed at testing the current protection circuit, requires a bench DC load connected to the EGSE switched power lines. The DC load allows to increment manually the amount of current to draw. By increasing slowly the current load up to the 2 A limit, the EPS protection circuit is expected to activate near the 2 A threshold by power-cycling the line until the over-current is removed.

The second test can be performed both by using the SPS or a bench power supply. The objective is to fully charge the battery, up to a voltage of 16.6 V. The EPS should react by cutting the input power, not allowing the battery to charge any further. When using a bench power supply, the maximum input current should not exceed 1 A, as stated in the EPS manual [8].

The bench DC load and the bench power supply used in these tests are shown in Figure 4.1a and 4.1b respectively.

(a) Bench DC load

(b) Bench Power Supply

Figure 4.1: Electric ground equipment.

Finally, the minimum voltage protection can be tested by simply letting the satellite drain the batteries. It can be sped up by using the Experiment simulators or the bench DC load as described before. The EPS circuit will enter SAFE mode, by cutting off the non-essential user lines. If the voltage drops even further, the EPS enters CRITICAL mode where all the user output are switched off. This process is described in Figure 4.2, where:

V_{max} = 16.6 V,
V_{safe} = 14.4 V,
$V_{critical}$ = 12.8 V,
V_{bat} = current voltage status.

These values are customizable [8].

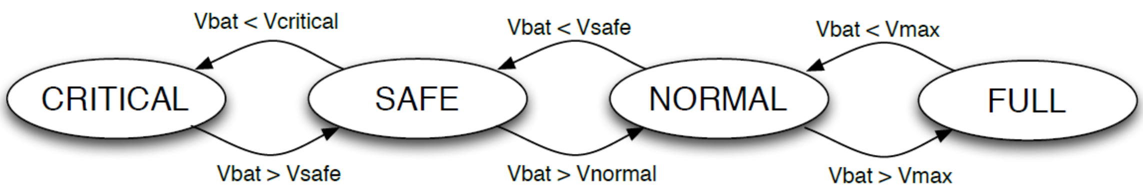

Figure 4.2: EPS voltage protection process

Because these tests are expected to provide a pass/fail result, there are no other expect outcomes. It is important, however, to note down any unexpected or unusual behaviour as well as logging the satellite's telemetry for further investigation and for future reference.

This test is a requirement for safely continuing to more complex tests.

4.3.2 Results

The maximum current protection was tested by slowly increasing the current draw from each of the switched line, using a bench DC load. The current was monitored by reading the telemetry value on the GoSH. The current reading shown in Figure 4.3, in the rightmost table, displays an intermediate value obtained during the test.

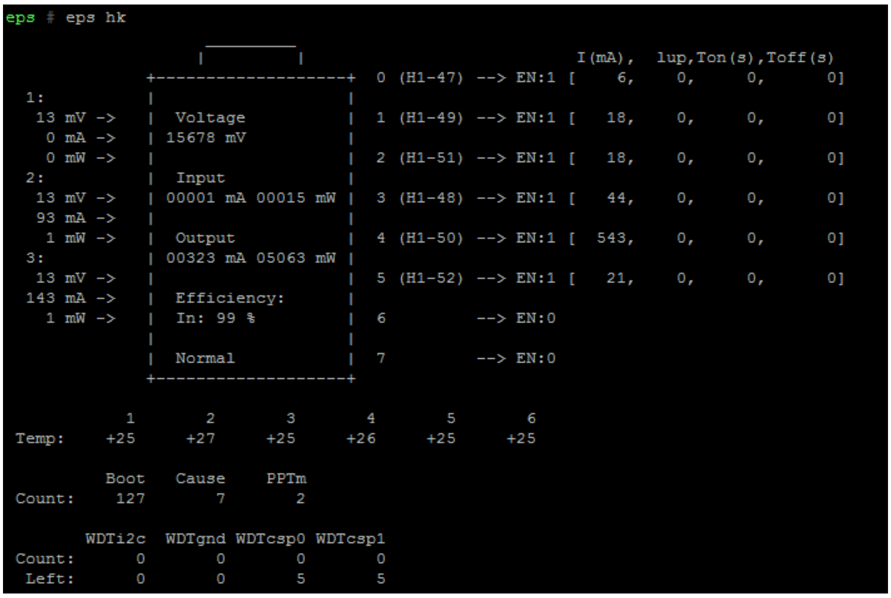

Figure 4.3: Gomspace SHell

The results of these tests are shown in Table 4.2

The results listed in Table 4.2 show that the current required to trigger the switched line interruption is slightly higher than the nominal of 2 A. However, this might be caused by calibration errors. Since the error it's smaller than 5% of the nominal value, so it should not be cause for concern. It was also noted that the trigger was not restarted when decreasing the current below 2 A, but it was necessary to set it back to zero. Finally, when applied a peak current of exactly 2 A, the trigger activates immediately, without showing the error

Switched Line	Voltage	Trigger Current
H1-47	5 V	Not used
H1-48	3.3 V	Not used
H1-49	5 V	2.10 A
H1-50	5 V	2.08 A
H1-51	5 V	2.06 A
H1-52	3.3 V	2.09 A

Table 4.2: Current limits

previously discussed.
The maximum battery voltage protection was tested during the fast charge test, described in Section 4.1. When the battery reached approximately 16.6 V, the input current was slowly reduced to zero, effectively reducing the input power to the minimum level to maintain a constant battery voltage. The telemetry of this test is shown in Figure 4.4a and Figure 4.4b.

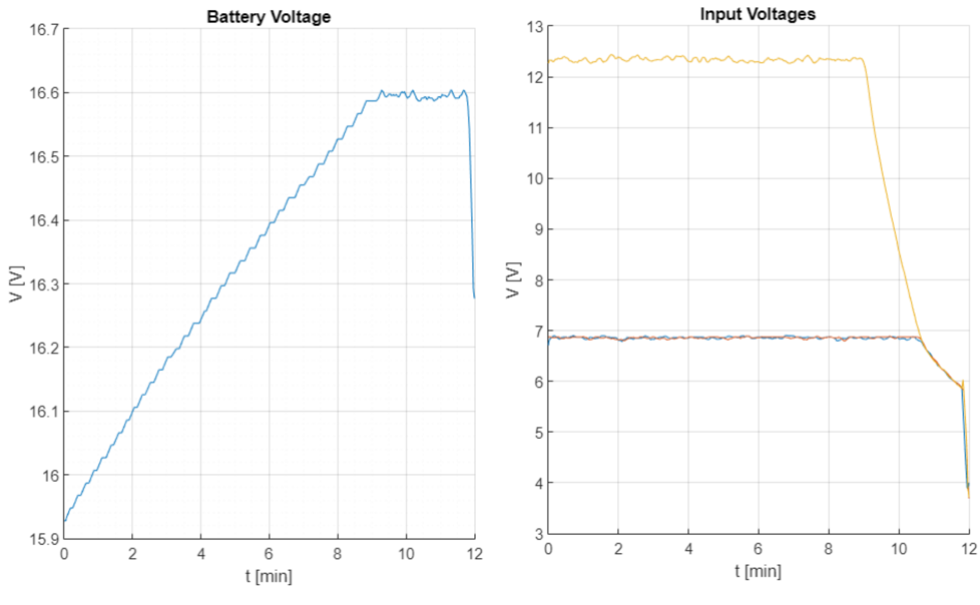

(a) Maximum V_{bat}

(b) Voltage drop due to V_{bat} protection activation

Figure 4.4: Maximum V_{bat} protection activation

Similarly, the minimum battery voltage protection was tested several times during the functional testing of the EPS, by allowing the satellite's subsystem to discharge the battery. Once the battery voltage reached the voltages described in Figure 4.2, it was possible to read the corresponding status from the GoSH, together with the switched line turning off as programmed.

4.4 Test Group 2 - No Experiments

4.4.1 Test Procedure

This test is used to evaluate the EPS capabilities when no experiments are used. Since SEUD and CUBES are expected to run continuously, the purpose of this test group is to evaluate the power status at the beginning of mission, immediately after deployment, when the experiments are not initialized yet, and to explore a possible operative case. This test group includes two subtests:

- Best Case Scenario,
- Worst Case Scenario,

with the details showed in Table 4.1. The best case is supposed to show how fast the battery can charge, in case of need. Since every experiment is turned off, the output power is be only caused to the satellite subsystems. Assuming the best solar flux, and no tumbling, the power balance is expected to be positive. This test aims at verifying this expectation, measure how much time the battery requires to be recharged in these conditions, and how the EPS reacts to this environment. In an operative framework, this test represent a mode used to quickly recharge the battery, i.e. in case of emergency or before running a power-heavy experiment more often than the expected schedule, such as NanoProp.
The worst case simulates the beginning of the mission, where the satellite has not deployed the antennas and the solar panels, and it's tumbling around all axes at the maximum rate suggested by the deployer, set to 5°/s. Furthermore, the minimum solar flux is assumed , thus the expected total input power is the lowest. The purpose of this test is to verify how much time the satellite can withstand this environment before entering CRITICAL mode. The satellite should be able to keep a nominal battery voltage for at least 30 minutes after deployment, as requested by most launch providers, before deploying the solar panels and the antennas.

The expectation of these tests is aimed at outlining the extreme cases, under the assumption that the intermediate test would not provide any more meaningful information. However, all the intermediate cases can be evaluated by the future Functional Test team by using the EPS testing framework described in this thesis work.

Since the most interesting outcome of these tests are related to the input power, these tests can be also used to verify the correct functionality of the SPS, by comparing the input power curves in each case with the theoretical ones, calculated by Gustav Pettersson [12]. These curves are shown in Figure 4.5a and 4.5b, and should be verified also on the following tests by using the post-processing tool, described in Section 4.2.

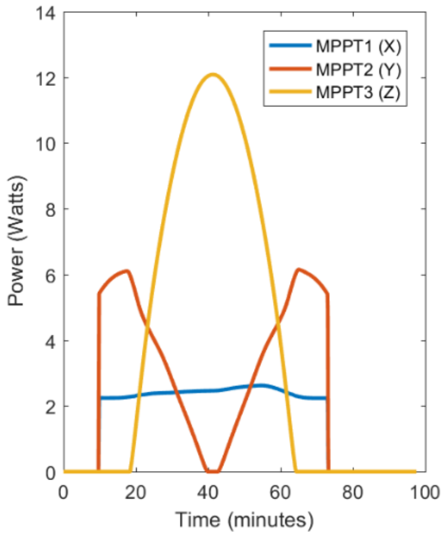

(a) Best case, nominal attitude

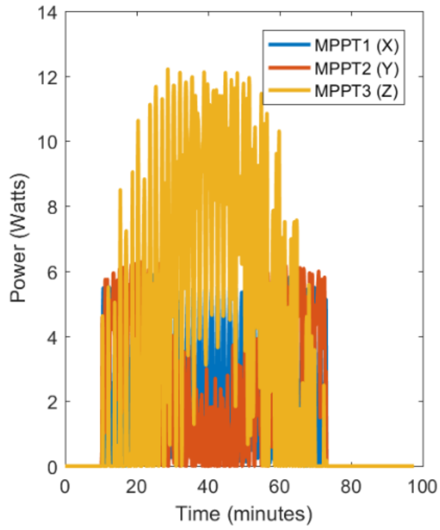

(b) Worst case, tumbling

Figure 4.5: Theoretical input power curves

4.4.2 Results

The following section shows the results of the test group running the satellite without experiments. First, the input power curve in Figure 4.6a and 4.6b shows the power input simulated by the SPS, both for the maximum and the minimum solar flux. It shows the satellite entering sunlight after approximately 11 minutes from the simulation start, reaching the maximum input power around 40 minutes and re-entering eclipse after 75 minutes. This curve matches very closely to the theoretical curve in Figure 3.6, proving that the SPS function properly for this test. The blue curve is MPPT1 (X), the red is MPPT2 (Y) and the yellow MPPT3 (Z)

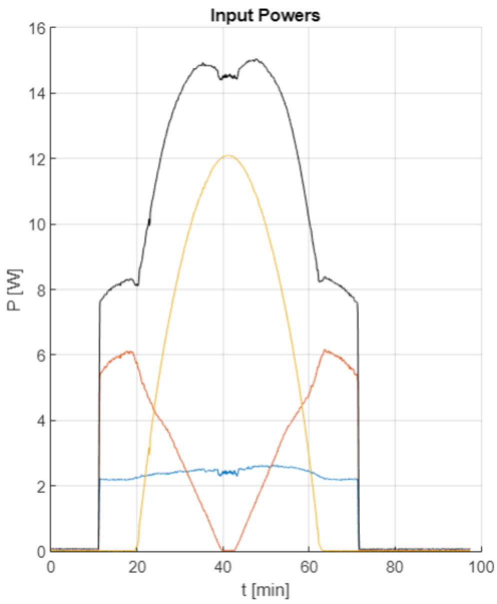

(a) Best flux, nominal attitude

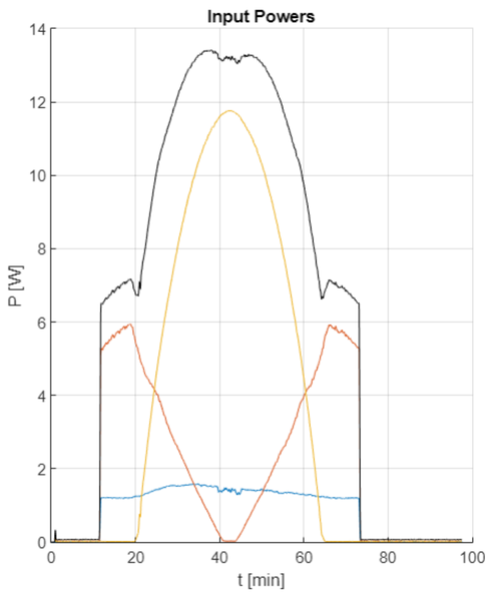

(b) Worst solar flux, nominal attitude

Figure 4.6: Theoretical input power curves

In Figure 4.7 and 4.8 are shown the system telemetry in the best case scenario, with maximum solar flux, no tumbling, and deployed solar panel configuration.

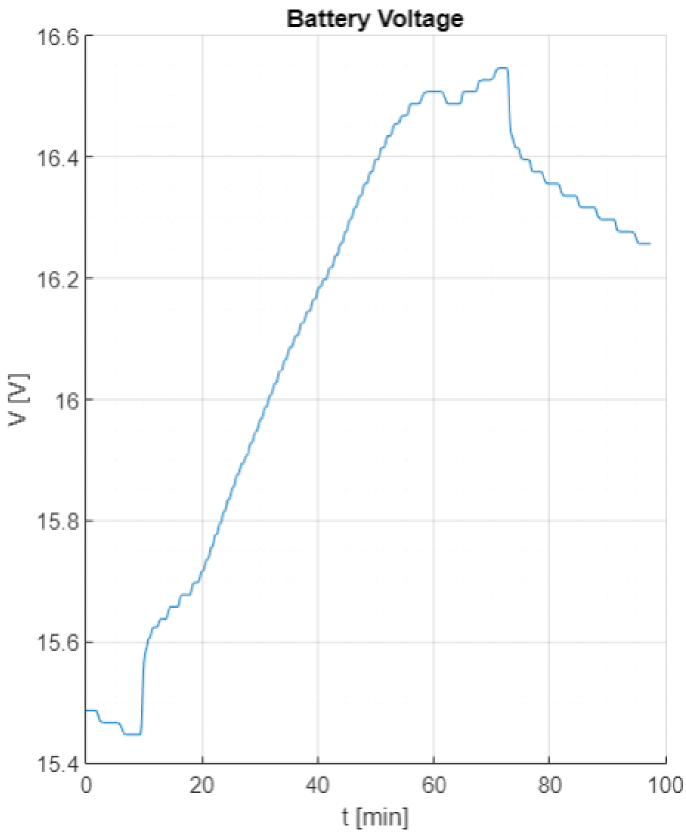

Figure 4.7: V_{bat}, no experiment, best case

Figure 4.7 shows that the battery voltage increases after one orbit with a ΔV of 0.77 V, demonstrating that the satellite will be able to recharge the battery after several orbits when no experiments are running. This could be useful in case the battery voltage would decrease under the NOMINAL threshold, requiring the satellite to stay idle until the batteries are recharged. The fast jumps in battery voltage correspond to the activation and deactivation of the SPS coinciding with the sunlight part of the orbit, in a process similar to the one described in the Appendix 3.4.

Figure 4.8 shows the system power draw of the satellite, which is calculated as $I_{SYS} \times V_{bat}$. Since there are no experiments running, this curve shows an approximate power consumption of the satellite's subsystems, where the iOBC, EPS are running and the iMTQ and the TRXVU are idle. The idle subsystems are correct for this test, where the radio communication is not expected and the iMTQ does not have to counteract any tumbling. This is why this curve is approximately constant between 2.7 W and 2.8 W, where the only significant variation is caused by the change in V_{bat}. It also shows the EPS keeping the system power as much constant as possible while V_{bat} changes, by changing I_{SYS}.

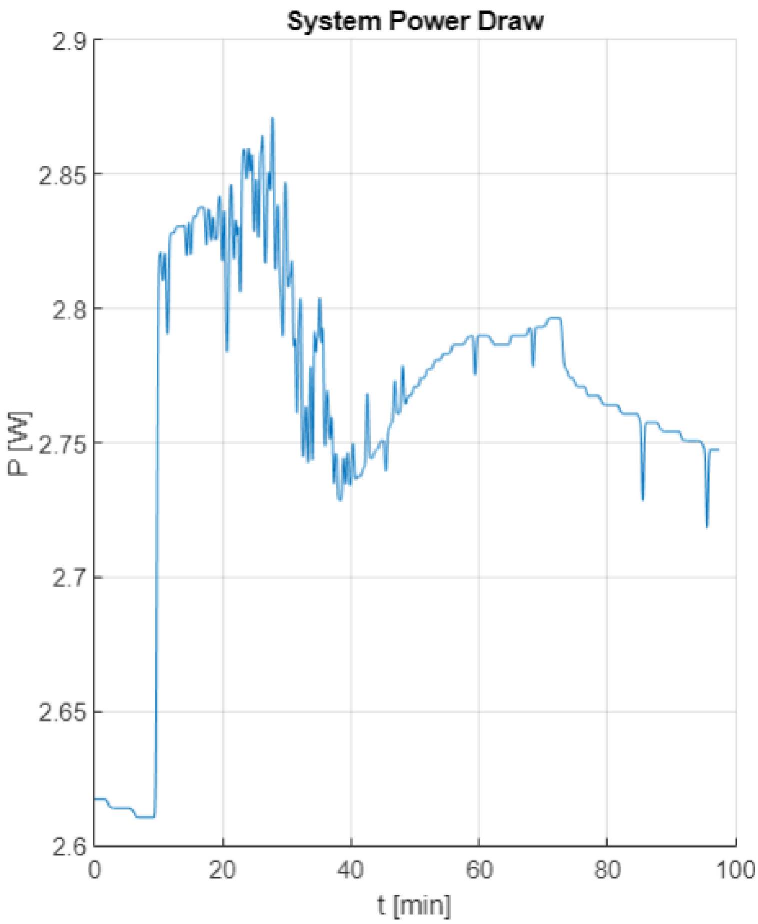

Figure 4.8: System Power, no experiments, best case

An increase of the battery temperature was recorded during the test. Figure 4.9 shows the temperatures recorded by four sensors on the battery pack. The increase in temperature is likely caused by the input buck converters.

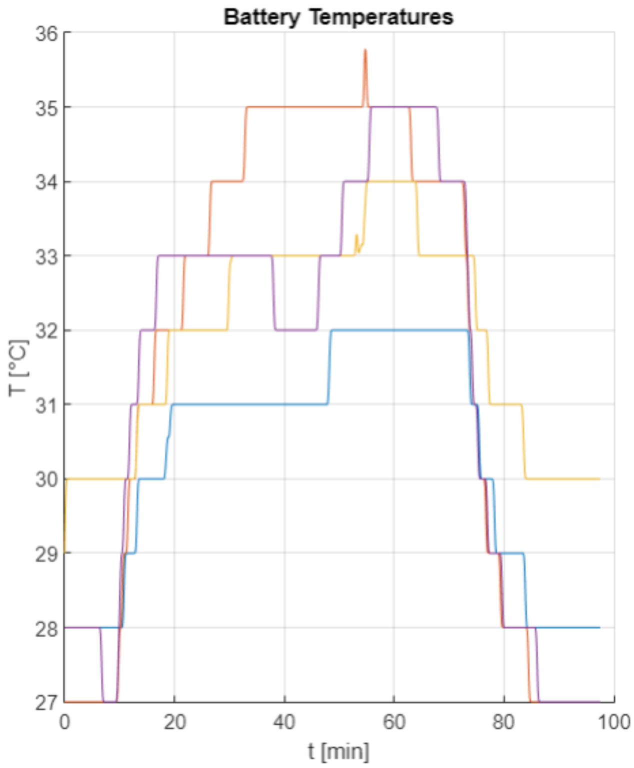

Figure 4.9: Battery temperatures, no experiments, best case

The absolute values of these temperatures are related to the room temperature where the test was conducted. The 10 °C peak increase, however, was reached in convecting environment, thus in space this temperature rise could be higher. Once in space, the only way the EPS can dissipate the heat is trough the CSKB and via radiation, on a smaller scale. Since the GOMspace EPS is a flight-proven product and the solar panel configuration was designed with respects to the EPS operative limits, this temperature raise is not a cause for concern. However, this effect should be taken into account by the Thermal team of the MIST, to improve the accuracy of the thermal model.

Figure 4.10 collect the battery voltage as described above, but in the worst case scenario, with the minimum solar flux, tumbling, and undeployed solar panel. This condition describe a worst-case deployment of the satellite, where MIST is expected to tumble at rates smaller than 5°/s and it is not allowed to activate any subsystem, including the HDRM and the AntS for the solar panels and antenna deployment.

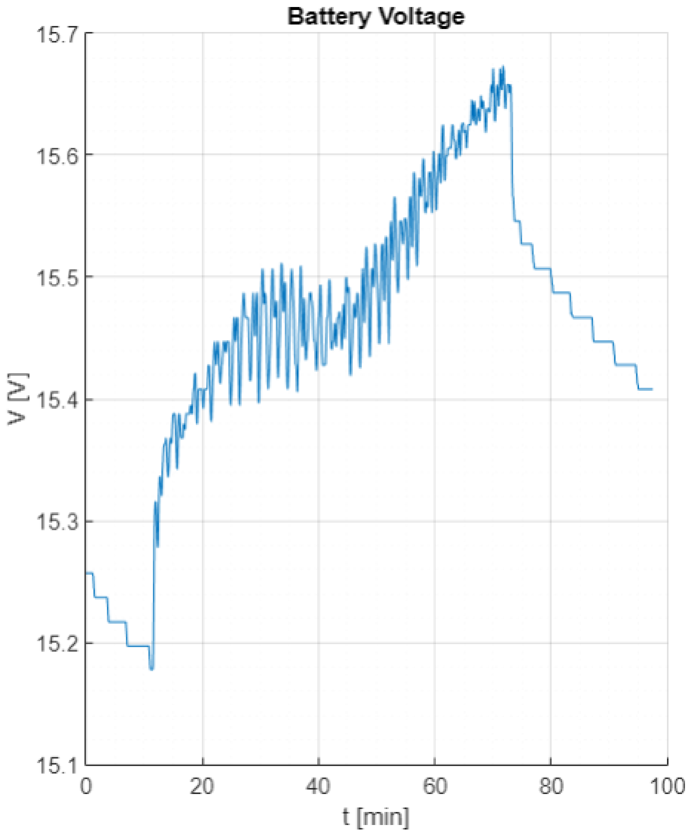

Figure 4.10: V_{bat}, no experiment, worst case

The battery voltage increases by 0.15 V over the course of one orbit. The noise introduced by the tumbling motion of the satellite is noticeable also in the battery charging pattern.

4.5 Test Group 3 - SEUD, CUBES

4.5.1 Test Procedure

The following test group involves the experiments that will run continuously during the satellite's operative life: SEUD and CUBES. According to the system budget document [17], these experiment can only be toggled on or off, resulting in a very simple power schedule, described in Table 4.3. These experiment are simulated via the experiment simulators and the MTI, described in Section 3.4.

Experiment	Power Consumption
SEUD	1 W
2x CUBES	2 x 1.3 W = 3.6 W

Table 4.3: CUBES and SEUD power consumptions [17]

SEUD is also used to handle the camera of the satellite. The camera can be considered as a subsystem of SEUD, thus its power consumption can be summed to SEUD, when the camera is expected to be active. The camera consumes about 0.6 W and runs for a few seconds [17]. The power schedule of SEUD and CUBES over the course of one orbit is summarized in Figure 4.11.

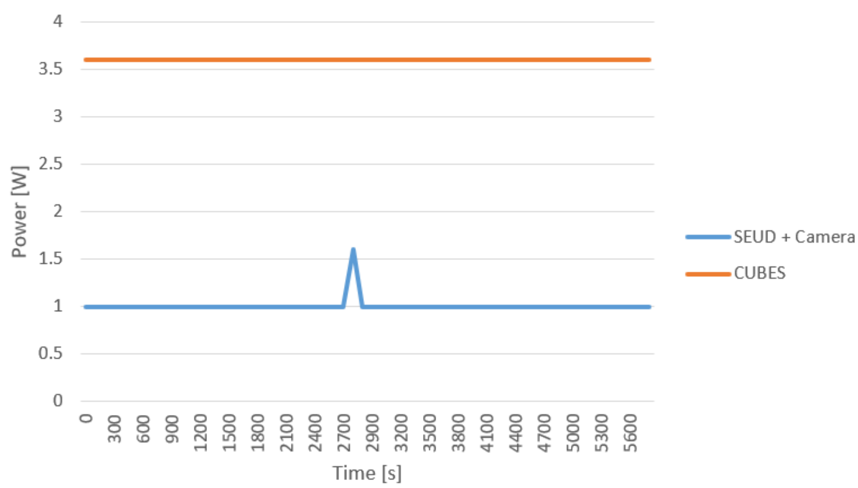

Figure 4.11: SEUD and CUBES power schedule

Because the experiments are always on, even during eclipse, this test group is expected to have in important impact on the battery voltage level. The system engineering simulations show a discharge rate of about 0.3 V/orbit [18]. It is also important to verify that the power consumption peak caused by the camera does not have any effect on the EPS. Finally, by comparing the voltage reading of the MTI logger and on the iOBC logger, it is possible to estimate the power loss caused by the experiment's harnessing.

4.5.2 Results

This test groups is based on the use of the MTI to manage the experiment simulators of SEUD and CUBES. These experiments present a simple power profile, as seen in Figure 4.11, but the amount of power required can be cause of concern for the battery voltage. In Figure 4.12 and 4.13 are shown the battery voltage profile during the test, in the best and worst case. The difference between these two cases is only in the solar flux, since in case of tumbling the experiments would not be activated. Appendix 6.4.2 contains the graphs not included in this discussion.

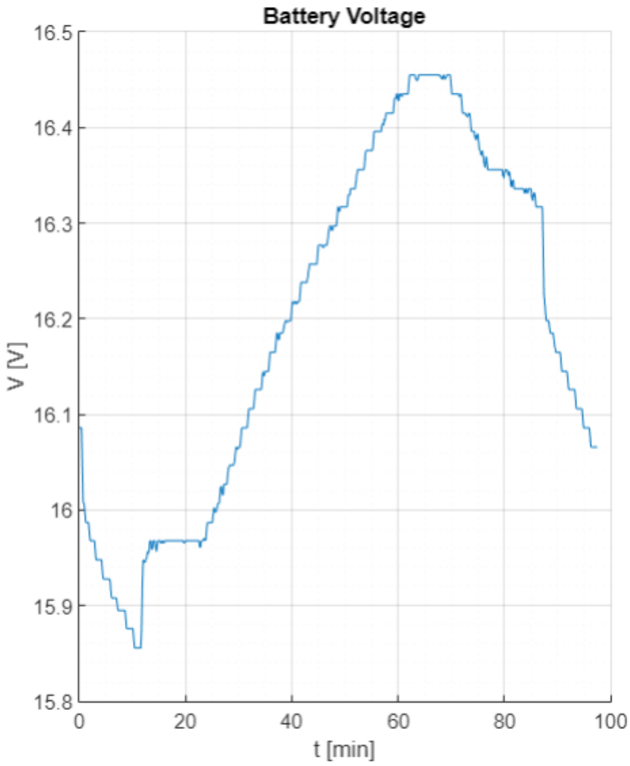

Figure 4.12: V_{bat}, SEUD and CUBES, best case

The battery voltage remains approximately the same between each orbit. By taking into consideration the additional consumption of the iMTQ and the TRXVU, it is safe to assume that the battery will uncharge on the following orbits, even when the solar flux is at his highest. It follows that the worst case scenario has a stronger impact on the battery voltage. Figure 4.13 shows a decay between orbits of -0.32 V, in accordance to the calculations from the System Engineering team [18].

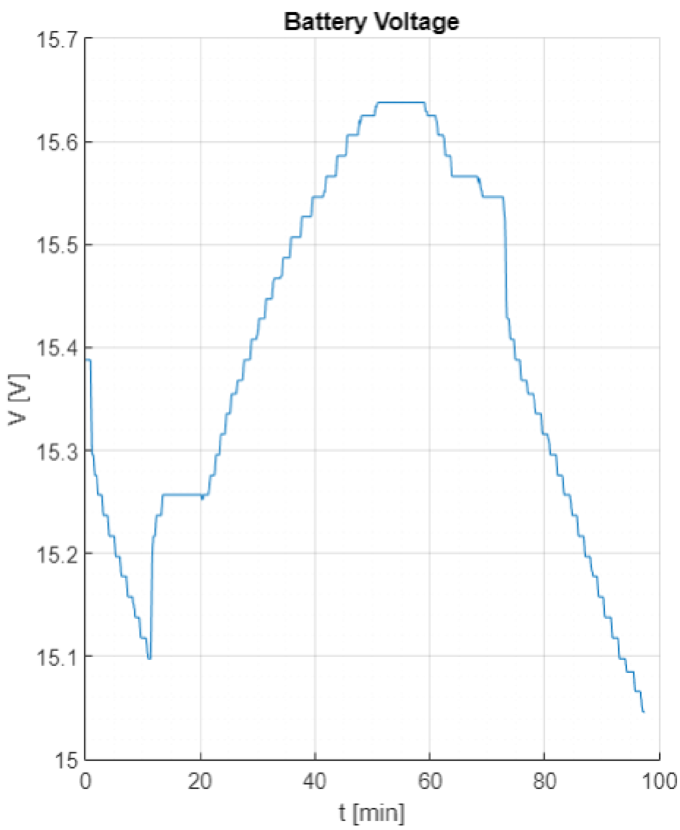

Figure 4.13: V_{bat}, SEUD and CUBES, worst case

This signifies that CUBES and SEUD should not be run at the same time during the lowest solar flux, and even in the highest solar flux they should be scheduled with times where the satellite is allowed to recharge the battery, similarly as tested in Section 4.4.

Figure 4.14 shows the power output measured by the iOBC on the switched power line for SEUD and CUBES experiment simulators.

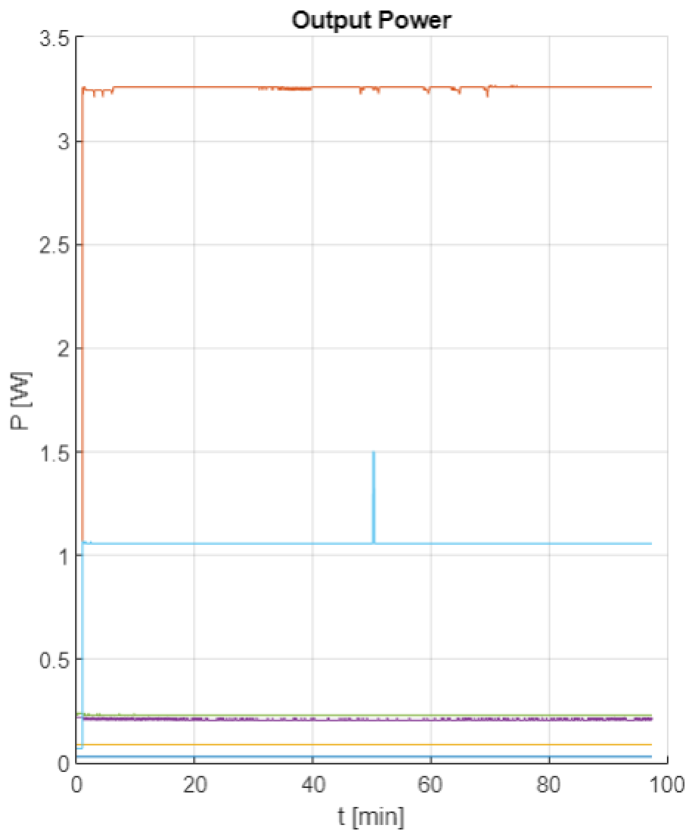

Figure 4.14: SEUD and CUBES, experiment simulators

Here the blue line represents SEUD, the spike is the camera activation, and the red line the combined power output of the two CUBES. The other lines represent noise from the other experiments, which are inactive. By comparing these values with the ones registered by the MTI, it is possible to estimate the power losses caused by the wires and the connectors, shown in Table 4.4.

Experiment	I	ΔV_{loss}	ΔP_{loss}
SEUD	0.282 A	-0.27 V	-0.066 W
SEUD + Camera	0.407 A	-0.39 V	-0.159 W
CUBES	0.615 A	-0.32 V	-0.197 W

Table 4.4: SEUD and CUBES wiring power losses

4.6 Test Group 4 - SEUD, SiC, PiezoLEGS

4.6.1 Test Procedure

This group of tests includes the experiments SEUD, SiC and PiezoLEGS. Contrary to SEUD, SiC and PiezoLEGS operate for a brief period of time and consume little power [17]. SiC is an integrated circuit board that is designed to provide power to PiezoLEGS, thus SiC must be turned on during the PiezoLEGS activation [17]. This is achieved by powering both experiments via the same switched line. However, since the MTI handles the two experiment simulators on different boards, its logger provides information about each experiment, while the iOBC is only be able to see the cumulative power draw of SiC and PiezoLEGS. Because of the low power consumption of these experiments, this test group is not expected to discharge the battery, however it is important to evaluate the power case where multiple experiments are connected to the same switched power line. Another purpose of this test is to evaluate the effect of a quick power load variations on the EPS. Similarly as before, the comparison between the two loggers allows the estimation of wire losses of these experiments.In Table 4.5, the power consumption of each experiment are summarized. As described before, SEUD is always running.

Experiment	Power Consumption	Running time	Scheduled
SiC standalone	0.42 W	1 s	Once every 60 minutes
PiezoLEGS	0.4 W	22 min	22 minutes before eclipse
SiC + PiezoLEGS	0.45 W	22 min	22 minutes before eclipse

Table 4.5: SiC and PiezoLEGS power consumptions [17]

Figure 4.15 shows an example of power schedule used for this test group. The time position of the camera activation (blue spike) is arbitrary, similarly for the SiC stand-alone activation, but separated 60 minutes from each others. Note that SiC and PiezoLEGS (red and yellow lines) power draw are seen from the satellite as one combined load, equivalent to the sum of the two.

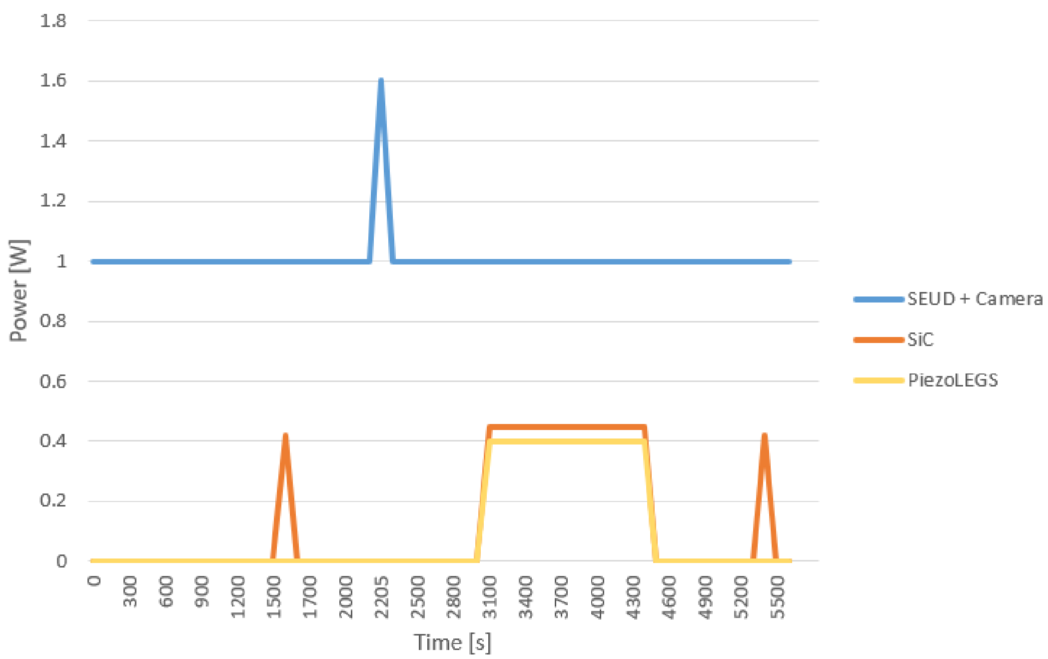

Figure 4.15: SEUD, SiC and PiezoLEGS power schedule

4.6.2 Results

This test group involved experiments with modest power draw. However, the PiezoLEGS requires the SiC board to be active when the experiment is running, thus these two experiments are placed on the same switched line. Consequentially, the power draw is the sum of these two. This test group is the most complex in terms of scheduling, so the preparation with the MTI must be done with care. The battery voltage during the orbit with best solar flux is shown in Figure 4.16.

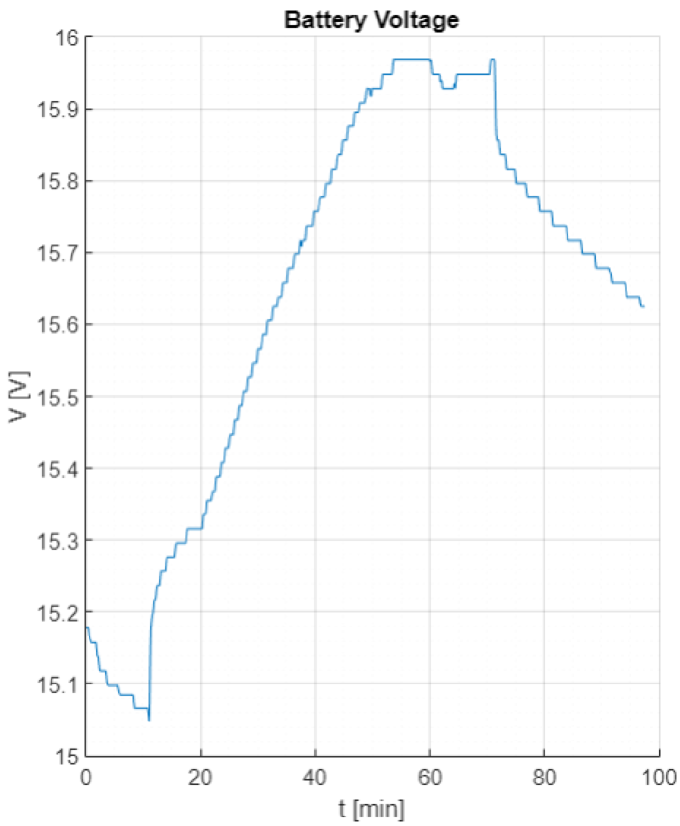

Figure 4.16: V_{bat}, SEUD, SiC and PiezoLEGS, best case

The total ΔV_{bat} for the best case is an increase of 0.45 V. The experiments do not have a strong impact on the battery voltage.

The battery voltage during the orbit with the worst solar flux is shown in Figure 4.17.

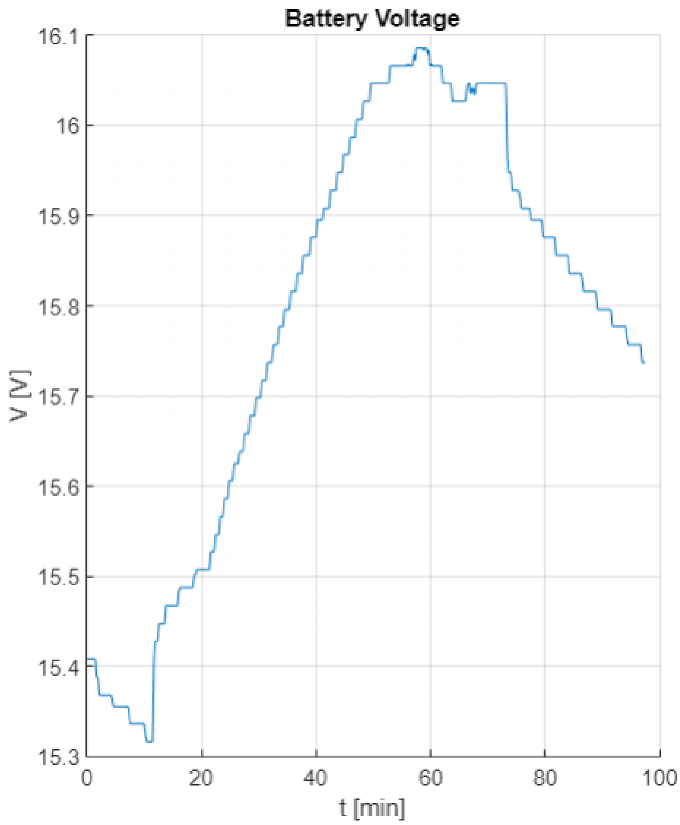

Figure 4.17: V_{bat}, SEUD, SiC and PiezoLEGS, worst case

Also in this case, the low power consumption of these experiments does not affect the battery state of charge dramatically. The ΔV_{bat} is 0.33 V.

Figure 4.18 shows the power output measured by the iOBC on the switched power line for SEUD and the joined switched power lines of SiC and PiezoLEGS experiment simulators.

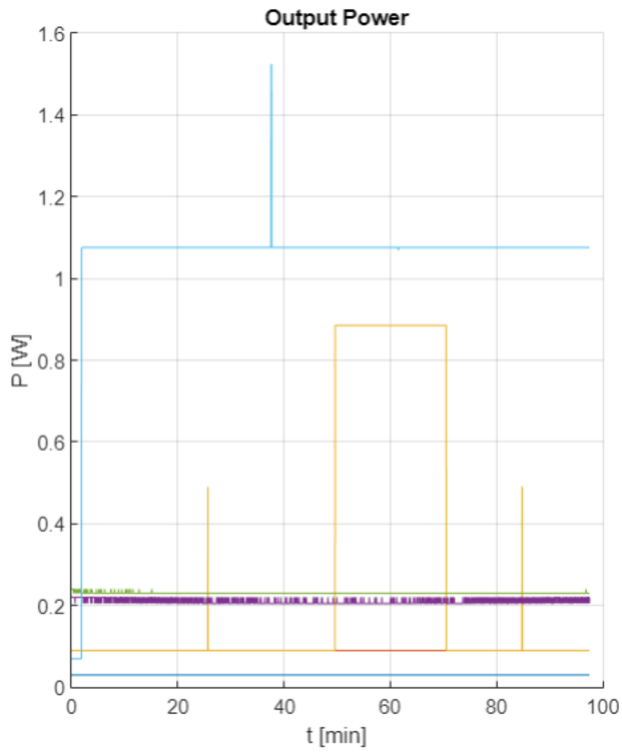

Figure 4.18: SEUD, SiC and PiezoLEGS, experiment simulators

Again here the blue line represents SEUD, while the yellow line correspond to the power draw from the switched line common for SiC and PiezoLEGS. The brief spikes 60 minutes apart represent the SiC activation, while the 20 minutes-long activation is caused by PiezoLEGS, which requires SiC to be activated at the same time. The other lines are the background noise of the other inactive experiments. The estimated power losses caused by wires and connectors are shown in Table 4.6.

Experiment	I	ΔV_{loss}	ΔP_{loss}
SiC	0.076 A	-0.08 V	-0.006 W
SiC + PiezoLEGS	0.069 A	-0.17 V	-0.025 W

Table 4.6: SiC and PiezoLEGS wiring power losses

4.7 Test Group 5 - SEUD, NanoProp

4.7.1 Test Procedure

The final test group includes SEUD and NanoProp. While SEUD operates as described before, NanoProp can be activated only once a day. It is a high power consumption experiment, requiring high power both for the pre-heating phase and during the thrust. However, since NanoProp's operation lasts for less than an hour and they are constrained by operating in sunlight, this test group is not expected to have a strong impact on the battery level. This expectation originates from the system engineering evaluations [18]. Its high power consumption, however, causes concerns in terms of the power distribution network. Furthermore, the power load is expected to happen in peaks, rather that slow increments, possibly causing brief interferences with other subsystems, as well as high losses in the satellite's harnessing, due to the wires diameter.
It is important to notice that the high power consumption will cause the resistors on the experiment simulators to overheat, thus cooling fans must be activated. In Table 4.7, the power consumption of each operative mode of NanoProp are summarized.

NanoProp Mode	Power Consumption	Running time	Scheduled
Tank Heating	1.7 W	40 min	On sunlight entry
Thruster Heating	1 W	100 s	28 min after sunlight entry
Thrust	6 W	10 min	After thruster heating

Table 4.7: NanoProp power consumptions [17]

Note that the tank heating will continue operating both during the thruster heating and ignition. This is justified by the need to keep the tank in a given temperature range for operating the thruster. This will result in a power consumption given by the sum of the heating and thruster power consumption, as shown in Figure 4.19. The beginning of the test after sunlight is also justified by thermal considerations [17].

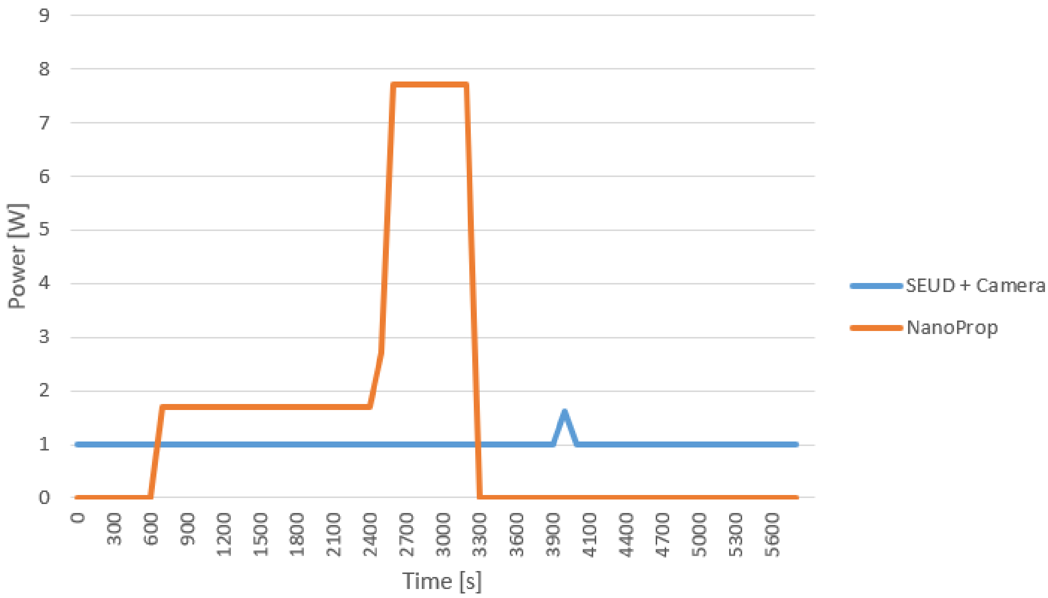

Figure 4.19: SEUD, SiC and PiezoLEGS power schedule

4.7.2 Results

The last test group includes the highest power consuming experiment: NanoProp. This propulsion experiment has an important power draw due to the use of heaters to keep the tank and the thruster to the correct temperature, as well as for thrusting. The tests, however, have been scheduled to happen only in sunlight, for thermal reasons, and maximum once a day. This means that, while the power draw would be higher than any other test group, it will also be brief and happen only when the satellite is powered by sunlight. The battery voltage during the orbit with the best solar flux is show in Figure 4.20.

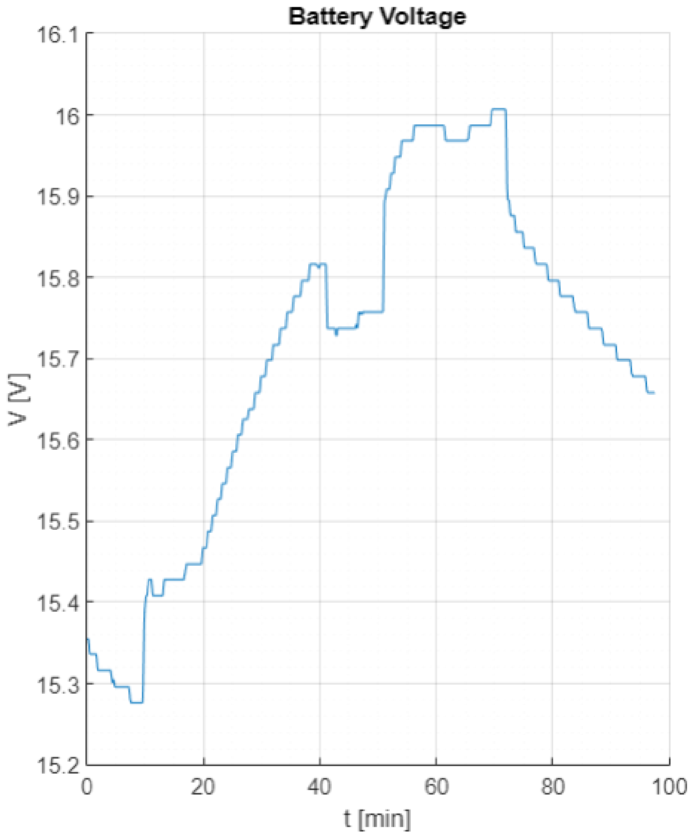

Figure 4.20: V_{bat}, SEUD, NanoProp, best case

The total ΔV_{bat} for the best case is an increase of 0.30 V. The experiment has a big impact on the battery SoC, albeit only for a short time. The battery charge is quickly recovered by the solar panel input, which reaches the maximum shortly after NanoProp has ceased its operations.

The battery voltage during the orbit with the worst solar flux is shown in Figure 4.21.

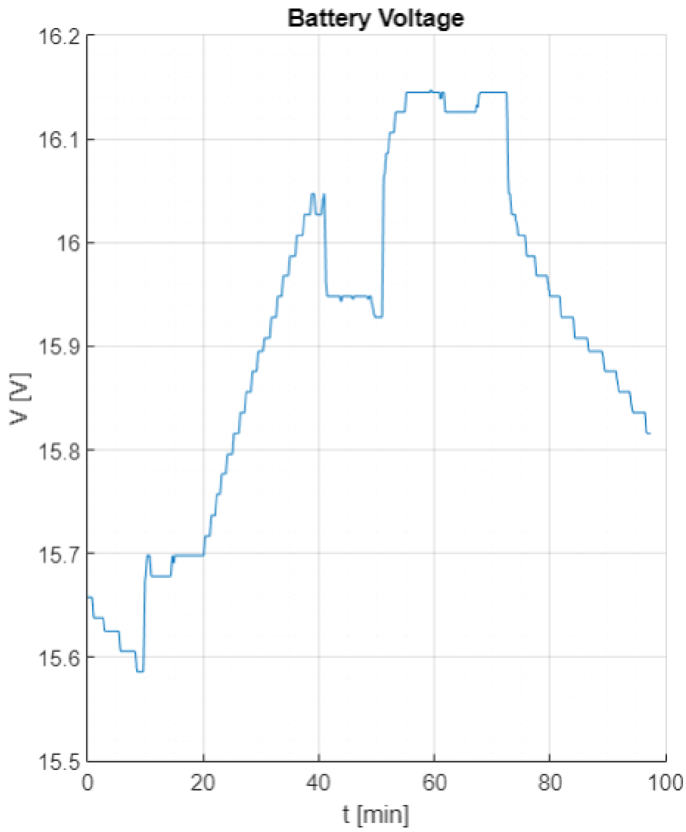

Figure 4.21: V_{bat}, SEUD, NanoProp, worst case

Similarly, the high consumption affects the battery voltage, but it's balanced by the peak input power. The ΔV_{bat} is lower with a gain of 0.16 V.

Figure 4.22 shows the power output measured by the iOBC on the switched power line for NanoProp and SEUD.

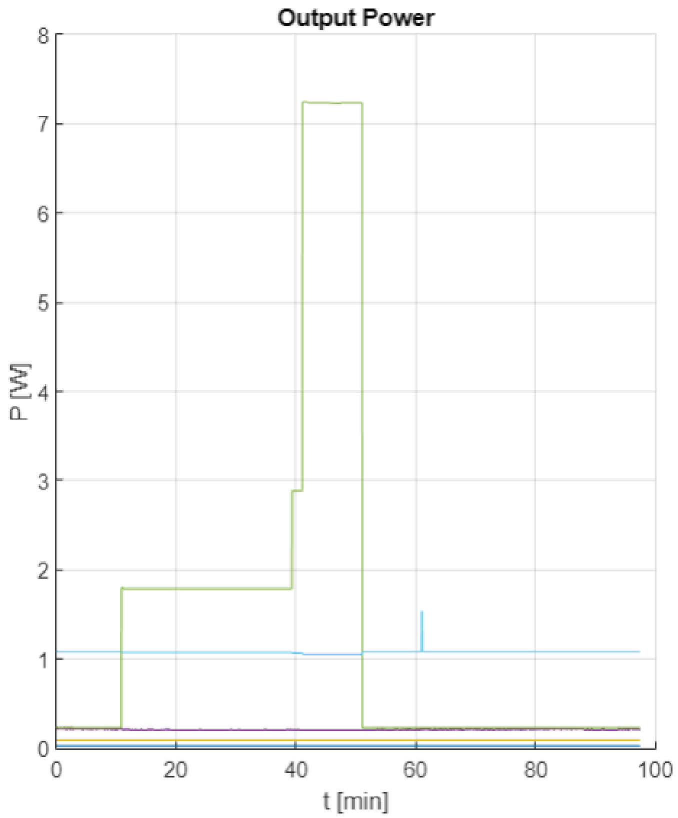

Figure 4.22: SEUD, NanoProp, experiment simulators

The blue line represents SEUD and the green line is NanoProp. The three operative phases of NanoProp are clearly seen on the curves, due to their high power consumption. It is possible to notice that, especially during the thrusting phase of NanoProp, the high power consumption also affects the voltage of the other switched lines, SEUD in this case. A magnified image is shown in Figure 4.23, where the small voltage drop is highlighted by the red circle.

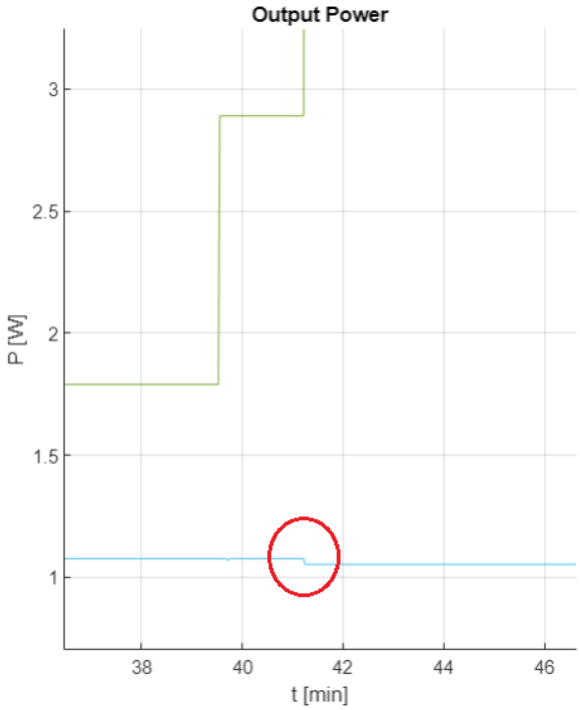

Figure 4.23: Voltage drop caused by the NanoProp thruster activation

The cause of this drop has to be investigated further. A possible explanation could be that the power distribution matrix of the EPS does not separate the switched lines properly, especially when high loads are applied. Alternately, a similar effect described in Appendix 6.2 could happen also within the CSKB. This would explain the similarity of the phenomenon. Also, since the CSKB pin are thicker than the experiment simulators wires, it would also explain why this happens on a very small scale.

The estimated power losses caused by the wires and the connectors are shown in Table 4.8. As expected from the high power drain of NanoProp, these losses are much more significant than in the previous test groups.

Experiment	I	ΔV_{loss}	ΔP_{loss}
Tank Heating	0.358 A	0.21 V	-0.1074 W
Thruster Heating	0.578 A	-0.36 V	-0.2081 W
Thrust	1.449 A	-0.84 V	-1.2172 W

Table 4.8: NanoProp wiring power losses

4.8 Test Ground 6 - Fast Charge and Discharge

4.8.1 Test Procedure

The last group of tests was designed to obtain a reference figure for fast charging and discharging operations of the satellite via the EGSE. The objective is to understand how fast the battery voltage increases and decreases when the input or output currents are close to the design limits, with a security factor of 10%. Table 4.9 shows the current and voltage used for these tests. The fast charge test was done via the manual control of the SPS [13], while the fast discharge used the experiment simulators maximum available current draw (L31), set via serial control. The three current and values for the charge test are for MPPT 1, 2 and 3, respectively, while for the discharge test they are relative to each switched line, also to the appropriate voltage.

Test Name	Current	Voltage
Fast Charge	0.9 A / 1.8 A / 0.9 A	7 V / 7 V / 12 V
Fast Discharge	Between 1 A to 1.5 A	3.3 V / 5 V

Table 4.9: Fast charge and discharge test values

4.8.2 Results

In Figure 4.24a and 4.24b the battery voltage increase and decrease are shown.

Using the data from these figures it's possible to obtain the maximum charge and discharge rates and their corresponding power input/output, shown in Table 4.10. The ratios have been calculated using only the linear part of the charging process, calculated as in Equation 4.1:

$$V/min = \frac{V_{max,linear} - V_{min,linear}}{t_{linear}} \quad , \tag{4.1}$$

Experiment	Input Power	Output Power	Maximum Rate
Fast Charge	26.55 W	0 W	0.064 V/min
Fast Discharge	0 W	16.35 W	-0.073 V/min

Table 4.10: Fast charge and discharge rates

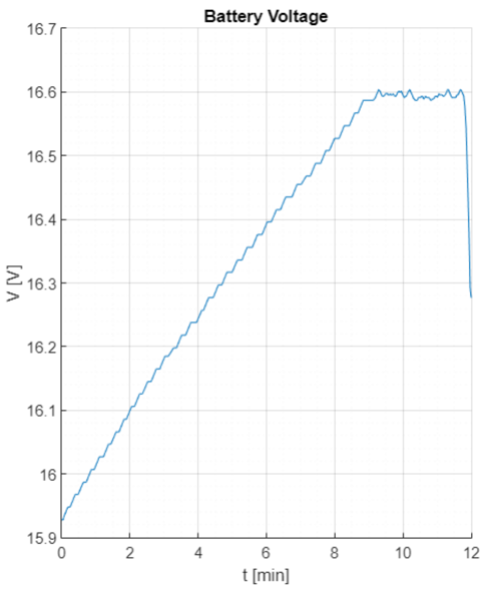

(a) V_{bat}, fast charge

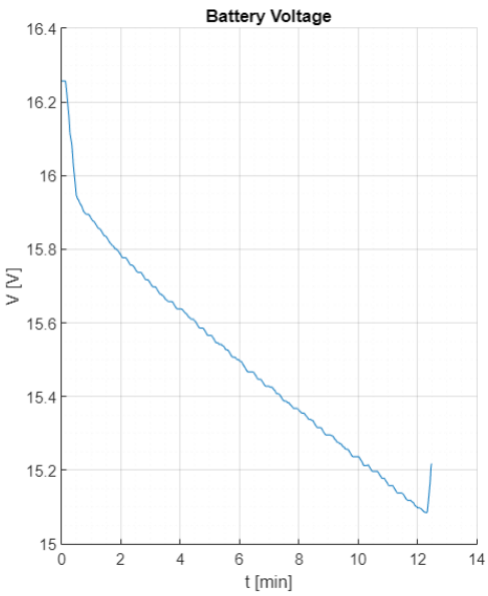

(b) V_{bat}, ast discharge

Figure 4.24: V_{bat}, fast charge and discharge

4.9 Found Issues

The graphs shown in previous sections contained filtered data, where spikes were hidden for graphical purposes. However, during some tests, it was noted that the iOBC would show an overflow on every variable saved on the SD card by the logger. These overflows appear without any apparent correspondence to other events happening in the satellite. Two examples are shown in Figure 4.25a and 4.25b. The input power value is the product of the input current and voltage, both saturated, while the switched line status is 1 for Nominal status, while the value 16 corresponds to the maximum binary value of the 4 bit variable size.

The source of these overflows was not found, but it affected all variables on random occurrence. They did not affect any of the satellite's functionalities. The WDT value read-out at the time of the overflow is is 269488144 (or hex 0x10101010), which is the same value observed during the WDT test [19], suggesting that these two types of overflow might be connected. Another possible cause is in the method used by the iOBC logger software in writing the variables on the memory (i.e. the overflow is only in the written variable, but not an actually registered value). This could be tested by searching for this

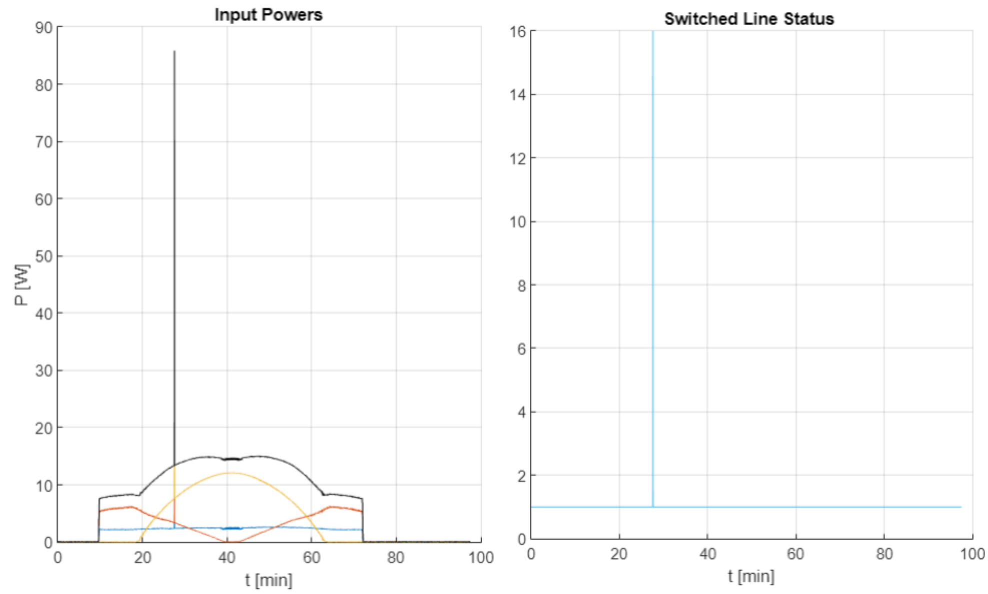

(a) Input power overflow

(b) Switched line status overflow

Figure 4.25: Some variables overflows

overflow with the flight software running on the iOBC.
Another issue is noticeable in Figure 4.18, as well as in all the other output power figures. While the active experiments should be the only ones drawing powers, it's seen that the other curves are resting at a non-zero value. This behaviour was suggested to be a calibration issue, since these curves appear also when the inactive experiments are physically disconnected. The non-zero value of power is probably caused by a non-zero reading of the current, that was noticed to oscillate in the range of 50 to 100 mA via the GOSH. More investigation is needed to explain this issue, including contacting the EPS manufacturer.

Chapter 5

Conclusions

5.1 Results Summary

In Section 4 the results obtained from the functional testing of the EPS have been presented. The outcome of each test proposed in Section 4.1 has been verified and commented. These results can be summarized in the following list:

- The testing framework for the EPS has been implemented successfully,
- The current and voltage protection systems functionalities have been verified,
- A fast charge and discharge pattern has been obtained,
- The system engineering simulations were confirmed in all the test cases,
- Every experiment group, with the exception of SEUD and CUBES, can be run without affecting the battery voltage over several orbits,
- SEUD and CUBES are the most power-intensive case, and they cause a progressive discharge of the battery over the course of one orbit,
- The power losses caused by the wires were measured,
- An increase in battery temperature has been measured,
- A variable overflow issue has been found.

These results can fill the testing requirement for the EPS, and the testing framework can be used to replicate these test on the full-scale flight simulations.

5.2 Future Steps

The methodology and the testing framework developed for this thesis work will allow the next Functional Test team to continue with investigating issues raised from these groups of tests as well as implementing the MTI testing framework for the full flight simulations. This includes running the tests again with the updated power draw values and schedules, finding the sources of the variable overflow and the non-zero current readings on inactive experiments.

A future development the framework could aim at improving the MTI GUI. This software has been written in MATLAB, but it could be made much lighter by creating a new version in C or Python. The removal of graphical object on demand could also allow the software to be less demanding in terms of required computational power.

Also the post processing tool used for the analysis of the results could be improved by integrating the splitting and data conversion process, as well as allowing more data to be visualized.

In case the real experiments will not be implemented by the time of the full orbital simulations, the experiment simulators should include the MSP, for example by connecting the Arduino Due MSP simulators to the experiment simulators. This would allow the iOBC to control the experiments. The MTI could be used to relay the commands from the Arduino Due to the experiment simulators, and to monitor and log the telemetry.

Finally, in preparation of the full orbital simulations, this testing framework can be used for IGIS, iMTQ and the TRXVU testing, to allow a characterization of the EPS in the complete subsystem stack.

Chapter 6

Appendix

6.1 Testing Framework

The experiments simulator's resistor network can be seen in an excerpt from the schematics, shown in Figure 6.1

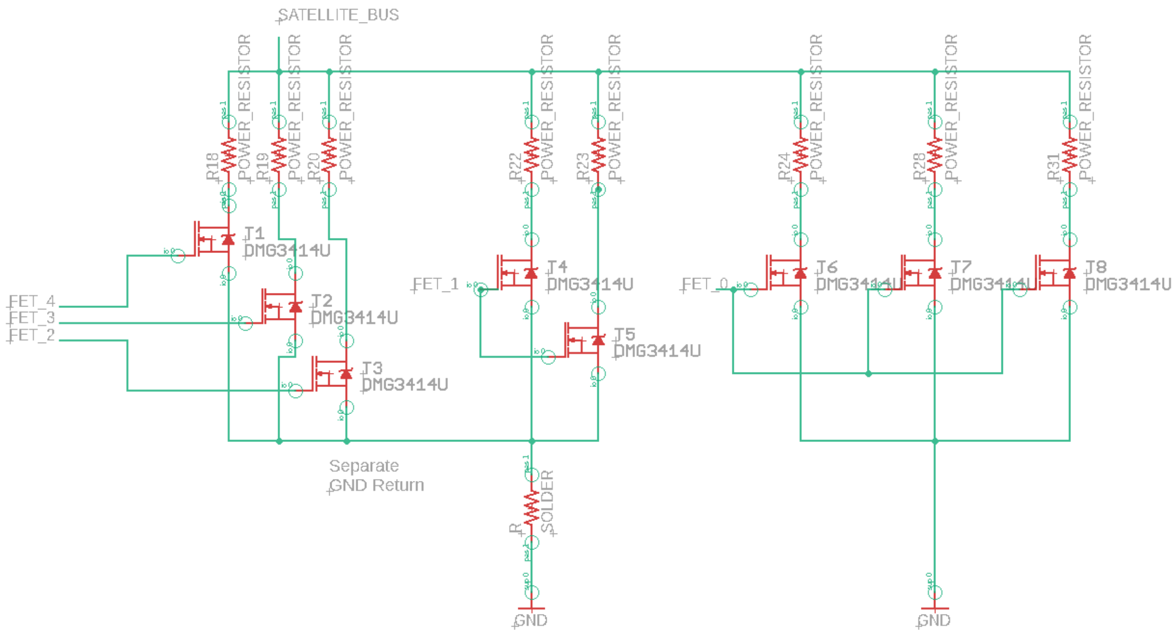

Figure 6.1: Schematics of the resistor network.

The complete EAGLE schematics and software of the Experiment Simulators is available on the MIST GitLab page: *https://gitlab.com/kth-mist/maltuino*

6.2 MIST Test Interface

To understand why the MTI is not able to measure the exact power consumption from the experiment simulators, the electric circuit that models their connection to the EPS is shown in Figure 6.2,

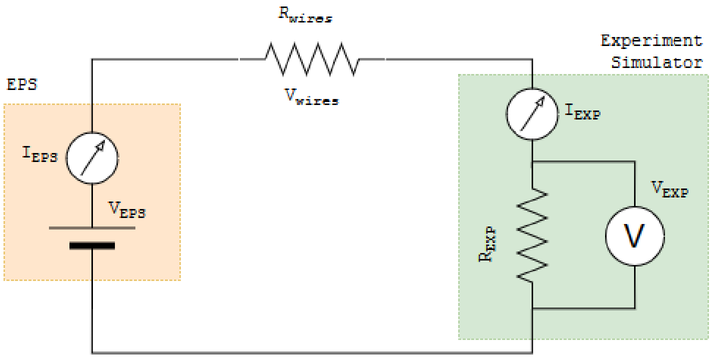

Figure 6.2: Simplified equivalent circuit of the experiment simulator / EPS connection.

where the EPS section is in orange and the experiment simulator in green. The EPS can provide the value of output power

$$P_{EPS} = I_{EPS}V_{EPS} \quad . \tag{6.1}$$

Because of the voltmeter and current sensor's positions on the board, the experiment simulators can not measure the losses caused by wiring, harnessing board and connections P_{wires}, but only the power dissipated in its part of the circuit. Since, according to Kirchhoff's voltage law,

$$\sum_i V_i = 0 \quad , \tag{6.2}$$

R_{wires} will cause a voltage drop, causing V_{EXP} to be lower than expected, thus P_{EXP} to appear incorrect. Also according Kirchhoff's current law, $I_{EPS} = I_{EXP}$, thus this value can be measured similarly by both sides.
According to Kirchhoff's voltage law, the result would be a mismatch between the power reading in the EPS and the experiment simulators. However, this mismatch can be used to estimate the power losses of the wires, assumed as a pure thermal dissipation:

$$P_{wires} = I_{EPS}^2 R_{wires} = I_{EXP}^2 R_{wires} \quad . \tag{6.3}$$

6.3 Test Procedure

Complete instruction list for a general EPS test procedure used in this thesis work.

- Before starting, check that the initial V_{bat} should be between 14.5 V and 15.5 V, to avoid triggering the EPS protection switches thus providing a good separation of causes during the test.

- *Check SD card*. The logger will append the new data to any existing log file, so the user shall backup any previous log file and delete it from the SD.

- *Check OBC software*. The latest version of the EPS logger (from the GitLab "functional-testing" repository) shall be compiled and ready to be run on the OBC.

- *Check SPS connections*. Make sure that the connections between the SPS and the EPS are correct and intact.

- *Power up SPS*. Use the provided power supplies to power up the SPS. Check their printed labels to make sure each SPS is powered by the correct source.

- *Open runRealtimeSPS and select the simulation data required for the test*. Use the MATLAB editor to modify the simulation data name to the appropriate one.

- *Run runRealtimeSPS*.

- *Start Eclipse*. Remove any previously running process.
- *Run the EPSlogger project*. Use the debug mode.

- *Open iOBC on COM4*.

- *Power up the satellite*.

- *Check that the logger is sending the live telemetry*.

- *Activate the MTI*.

- *Check the process*. The values of V_{bat} should be under control at all time and shall be compared from the logger with a multimeter connected to the EGSE. Also check that MPP voltage and current match between the logger, the SPS and the MATLAB software.

6.4 Results

In this section are shown some graphs obtained during the tests but not used to draw conclusions.

6.4.1 Test Group 2 - No Experiments

Figure 6.3 shows the input power curve obtained from the SPS tumbling profile. The oscillating nature of this curves reflect the tumbling motion of the satellite, and match the theoretical curve in Figure 4.5b. The average input power is 3.68 W, versus a system power consumption of 2.68 W, justifying a positive ΔV_{bat}. Similar patterns are followed by the battery temperatures, in Figure 6.5.

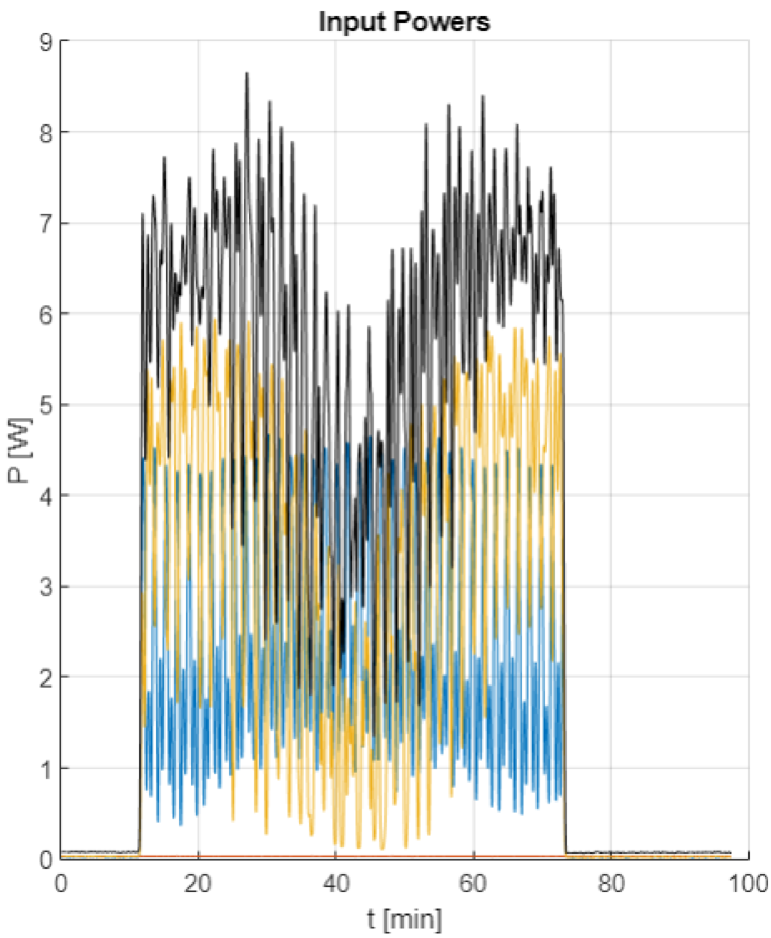

Figure 6.3: Input Power, no experiments, worst case

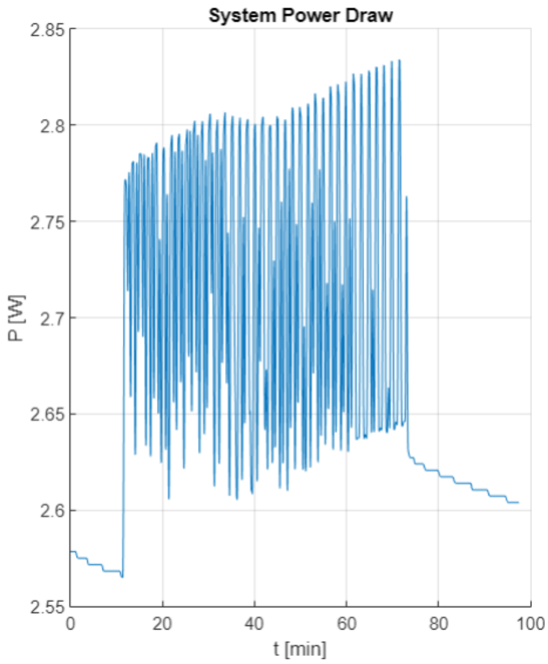

Figure 6.4: System Power, no experiments, worst case

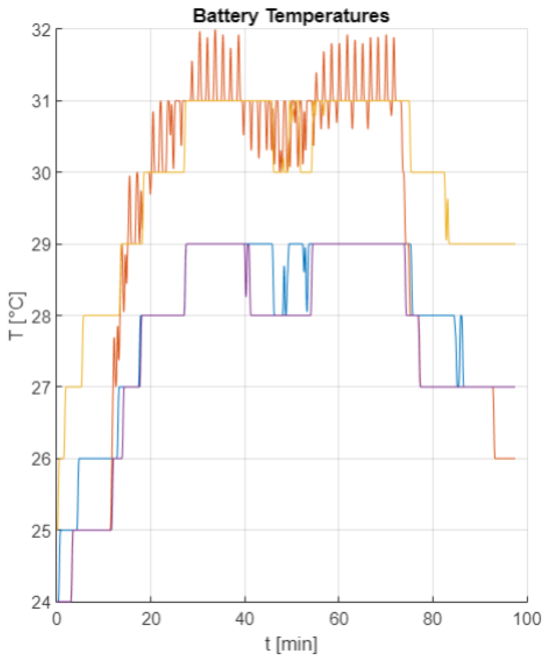

Figure 6.5: Battery temperatures, no experiments, worst case

6.4.2 Test Group 3 - SEUD, CUBES

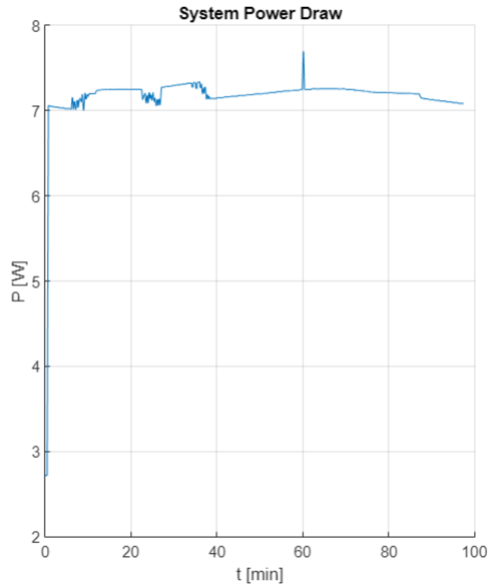

(a) Best solar flux

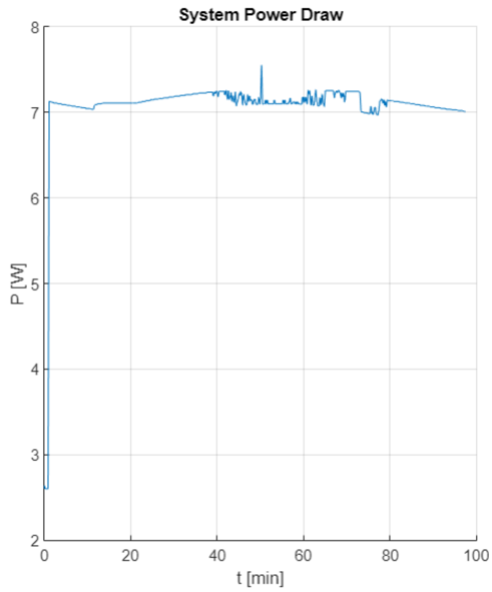

(b) Worst solar flux

Figure 6.6: System Power, SEUD and CUBES

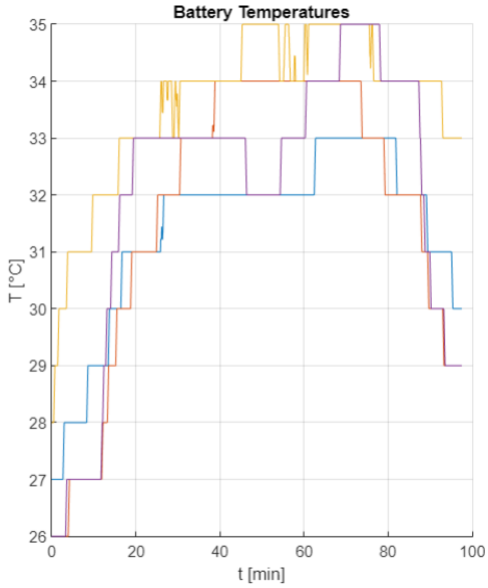

(a) Best solar flux

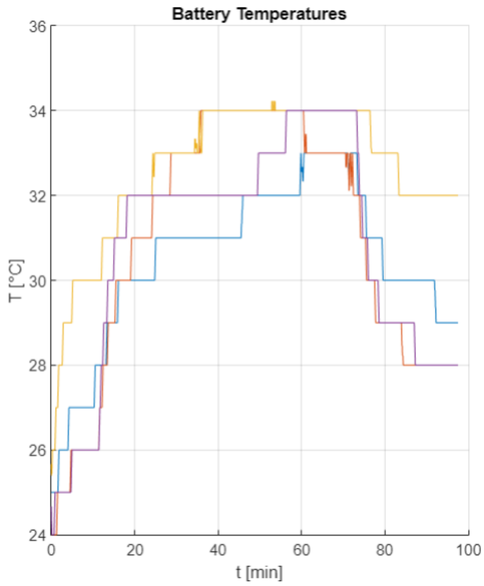

(b) Worst solar flux

Figure 6.7: Battery temperatures, SEUD and CUBES

6.4.3 Test Group 4 - SEUD, SiC, PiezoLEGS

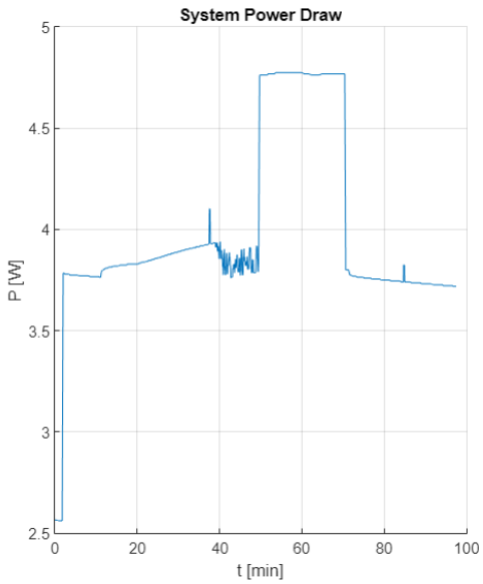

(a) Best solar flux

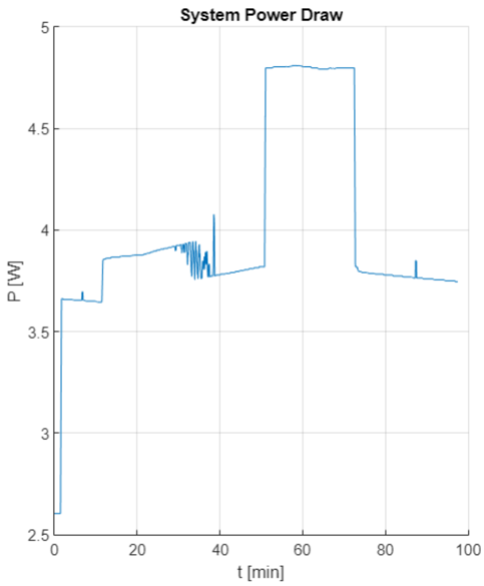

(b) Worst solar flux

Figure 6.8: System Power, SEUD, SiC and PiezoLEGS

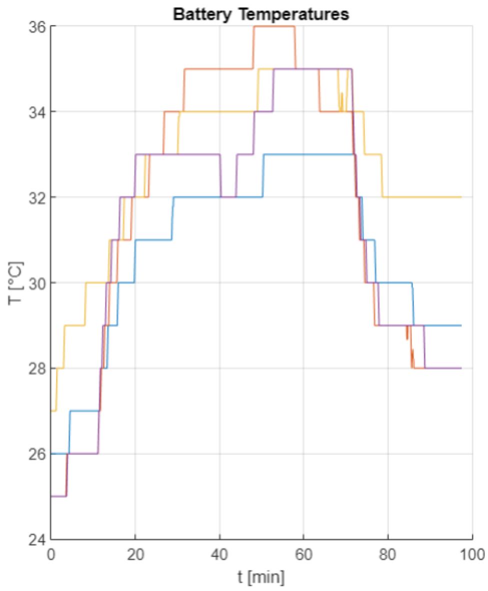

(a) Best solar flux

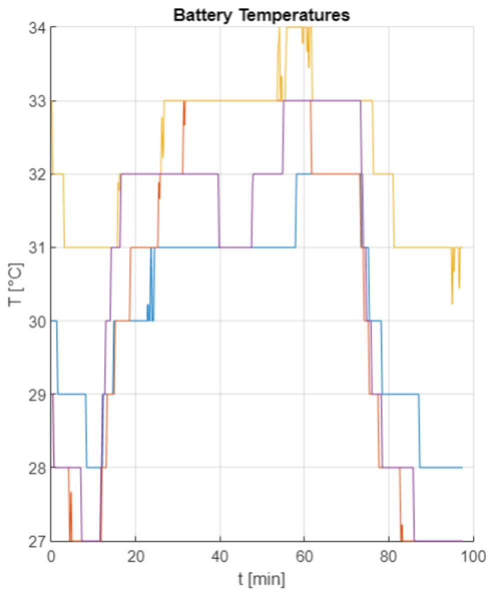

(b) Worst solar flux

Figure 6.9: Battery temperatures, SEUD, SiC and PiezoLEGS

6.4.4 Test Group 5 - SEUD, NanoProp

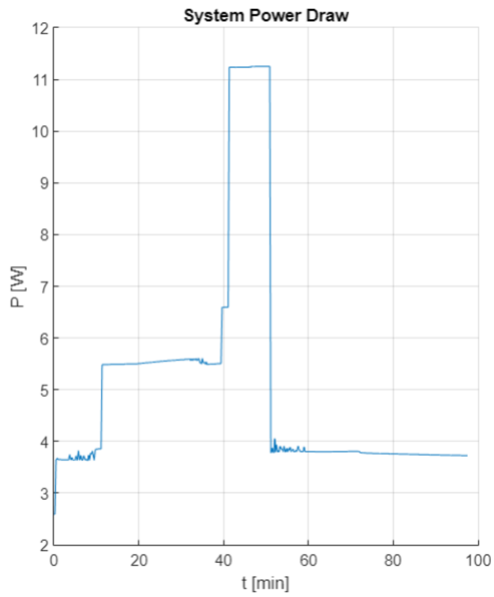

(a) Best solar flux

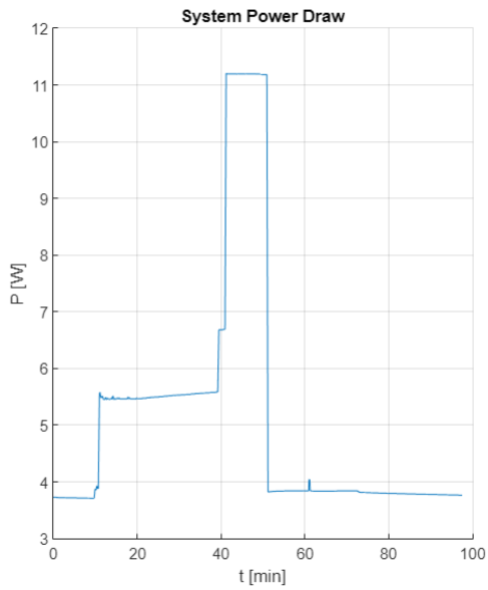

(b) Worst solar flux

Figure 6.10: System Power, SEUD, NanoProp

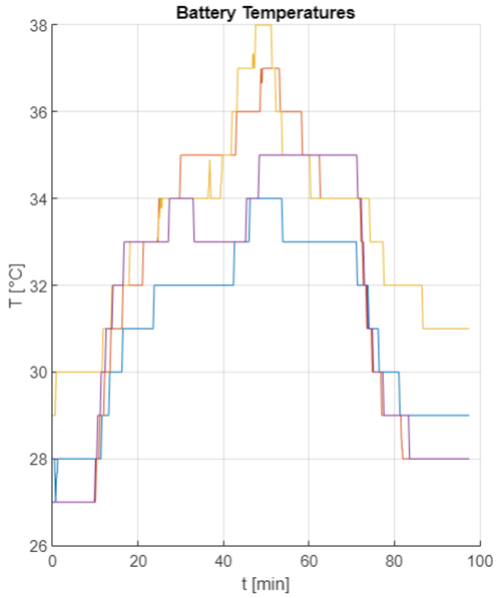

(a) Best solar flux

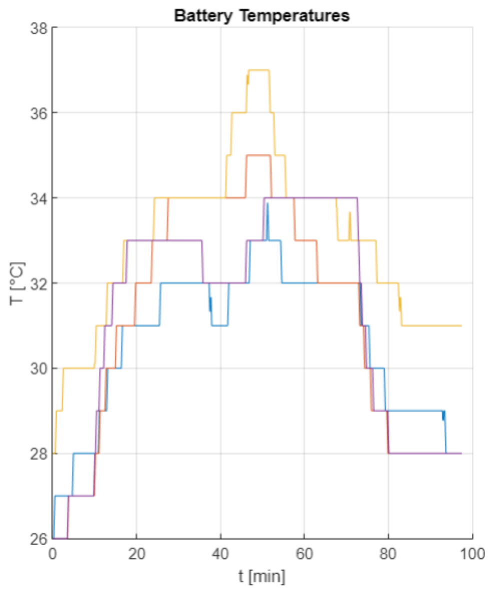

(b) Worst solar flux

Figure 6.11: Battery temperatures, SEUD, SiC and PiezoLEGS

Bibliography

[1] Cal Poly SLO The CubeSat Program. "CubeSat Design Specification". In: *The CubeSat Program, Cal Poly SLO* Rev. 13 (2014), pp. 4711–4721.

[2] Alessandra M. Brandão Fernando T. Bueno Thyrso Villela Cesar A. Costa and Rodrigo Leonardi. "Towards the Thousandth CubeSat: A Statistical Overview". In: *International Journal of Aerospace Engineering* (2019), p. 13.

[3] Sven Grahn. *MIST - The Miniature Student Satellite - Basic Facts*. 1999. URL: `https://mistsatellite.space/basic-facts/` (visited on 05/03/2019).

[4] Jasper Bouwmeester Martin Langer. "Reliability of CubeSats – Statistical Data, Developers' Beliefs and the Way Forward". In: Annual AIAA/USU Conference on Small Satellites. 2016.

[5] Dr. K.V.K.K. Prasad. *ISTQB Certification Study Guide*. Wiley, 2008.

[6] Annam Tanveer. *M510-006 MIST Project Handbook*. Version 5. KTH Space Center, 2017.

[7] ESA. *Onboard Computers*. 2019. URL: `https://www.esa.int/Our_Activities/Space_Engineering_Technology/Onboard_Computer_and_Data_Handling/Onboard_Computers` (visited on 05/10/2019).

[8] *NanoPower P31u/P31us Manual*. Version 1. GOMspace.

[9] Stuart Bowden Christiana Honsberg. *IV Curve*. URL: `https://www.pveducation.org/pvcdrom/solar-cell-operation/iv-curve#footnoteref1_hi3xyjk` (visited on 05/13/2019).

[10] Sven Grahn. *M132-006 MIST Solar Cell Configuration*. Version 1. KTH Space Center, 2017.

[11] Malte Gruber. "Functional Testing of the MIST Satellite". In: (2018).

[12] Gustav M. Pettersson. “Solar Panel Simulation for Testing of Nanosatellite Power Systems”. In: (2018).

[13] Gustav M. Pettersson. *Solar Panel Simulator*. URL: `https://github.com/gustavmpettersson/Solar-Panel-Simulator/` (visited on 06/04/2019).

[14] *ISIS EPS-EGSE User Manual*. Version 2. ISIS.

[15] Prashant Yadav Stefano Barra. *M631-021 EPS Watchdogs*. Version 1. KTH Space Center, 2019.

[16] European Coordination for Space Standardization. “Space Engineering - Testing”. In: *ECSS* ECSS-E-ST-10-03C (2012).

[17] Sven Grahn. *M542-017 MIST Power Schedule*. Version 3. KTH Space Center, 2019.

[18] Anna Larsson. *M540-002 System engineering and power and memory budgets*. Version 1. KTH Space Center, 2019.

[19] Theodor Stana. *M631-008 EPS Watchdogs*. Version 2. KTH Space Center, 2019.

TRITA-EECS-EX-2019:570
www.kth.se